BMC Clinical Pharmacology

BioMed Central

Research article

The pharmacokinetics of the interstitial space in humans

David G Levitt*

Address: Department of Physiology University of Minnesota

Email: David G Levitt* - levit001@umn.edu

* Corresponding author

Published: 30 July 2003

BMC Clinical Pharmacology 2003, **3**:3

Received: 17 April 2003

Accepted: 30 July 2003

This article is available from: http://www.biomedcentral.com/1472-6904/3/3

Abstract

Background: The pharmacokinetics of extracellular solutes is determined by the blood-tissue exchange kinetics and the volume of distribution in the interstitial space in the different organs. This information can be used to develop a general physiologically based pharmacokinetic (PBPK) model applicable to most extracellular solutes.

Methods: The human pharmacokinetic literature was surveyed to tabulate the steady state and equilibrium volume of distribution of the solutes mannitol, EDTA, morphine-6-glucuronide, morphine-3-glucuronide, inulin and β-lactam antibiotics with a range of protein binding (amoxicillin, piperacillin, cefatrizine, ceforanide, flucloxacillin, dicloxacillin). A PBPK data set was developed for extracellular solutes based on the literature for interstitial organ volumes. The program PKQuest was used to generate the PBPK model predictions. The pharmacokinetics of the protein (albumin) bound β-lactam antibiotics were characterized by two parameters: 1) the free fraction of the solute in plasma; 2) the interstitial albumin concentration. A new approach to estimating the capillary permeability is described, based on the pharmacokinetics of the highly protein bound antibiotics.

Results: About 42% of the total body water is extracellular. There is a large variation in the organ distribution of this water – varying from about 13% of total tissue water for skeletal muscle, up to 70% for skin and connective tissue. The weakly bound antibiotics have flow limited capillary-tissue exchange kinetics. The highly protein bound antibiotics have a significant capillary permeability limitation. The experimental pharmacokinetics of the 11 solutes is well described using the new PBPK data set and PKQuest.

Conclusions: Only one adjustable parameter (systemic clearance) is required to completely characterize the PBPK for these extracellular solutes. Knowledge of just this systemic clearance allows one to predict the complete time course of the absolute drug concentrations in the major organs. PKQuest is freely available http://www.pkquest.com.

Background

The distribution of most hydrophilic solutes (e.g. β-lactam antibiotics) is limited to the extracellular space because of their cell membrane impermeability. Thus, the pharmacokinetics of this large class of compounds is determined primarily by the volume of distribution and the kinetics of exchange with the interstitial space. Given the general importance of this class of drugs, there has been surprisingly little analysis of the pharmacokinetics of the interstitial space in humans. The 1959 review article by Edelman et. al. [1] remains the standard reference on the extracellular space. In addition, there are two extensive

reviews of the structure and function of the interstitial space [2,3].

An accurate pharmacokinetic description of the interstitial space is essential for the development of a physiologically based pharmacokinetic model (PBPK) for extracellular solutes. Although PBPK models have been used extensively to describe human pharmacokinetics, nearly all of these studies have involved solutes that have intracellular distributions, and, thus, do not require detailed modeling of the interstitial space. One exception is the recent application of PKQuest to the extracellular solutes inulin and the beta-lactam antibiotics [4]. PKQuest is a new PBPK program that has been applied to the human pharmacokinetics of a large number of solutes [4–8]. Although the agreement between the PKQuest PBPK model predictions and the experimental data for these extracellular solutes was satisfactory, subsequent application of PKQuest to other extracellular solutes demonstrated that there was a small, but systematic, error in the PKQuest predictions. This error is the stimulus for this more in depth analysis of interstitial pharmacokinetics.

Probably the most detailed application of a PBPK model to an extracellular solute is the study of Tsuji et. al. [9] of the pharmacokinetics of cefazolin in the rat. In this investigation, nearly every PBPK parameter required by the model was directly measured, including organ blood flows and weights, renal and hepatic clearance and the time dependence of cefazolin concentration in the different organs. Tsuji et. al. [9] estimated interstitial volumes from measurements of the steady state inulin tissue concentrations. The interstitial volumes in the original PKQuest PBPK model were based on these inulin volumes of Tsuji et. al. [9] scaled to give the correct total volume in humans. As will be shown below, inulin is not a good solute to use to measure interstitial volume and this probably contributed to the error in the earlier PKQuest PBPK predictions.

Methods

All the experimental data were obtained from earlier publications. In most cases, the published data represented the average of the experimental measurements in a number of subjects and it was assumed that it represented one "average" subject. In a few cases (indicated by a N = 1 in Table), data for a single subject were published and used in the calculations. The program UN-SCAN-IT (Silk Scientific Corporation) was used to read the data from the published figures. Most of the figures shown in this paper are direct copies (in jpeg format) of standard PKQuest output.

Measurement of steady state volume of distribution (V_{ss})

To ensure that a consistent calculation of V_{ss} was used, all the values of V_{ss} were recalculated by applying PKQuest [8] to the published venous concentration data. In this calculation, deconvolution of the intravenous input is used to find the 2 or 3 exponential unit dose bolus response function r(t):

$$r(t) = \sum_{i=1}^{P} B_i e^{-t/T_i} \quad (1)$$

The expression for V_{ss} is then found from the area under the curve (AUC) and mean residence time (MRT) for this r(t) (for unit dose):

$$V_{ss} = MRT / AUC = \sum_{i=1}^{P} B_i T_i^2 / (\sum_{i=1}^{P} B_i T)^2 \quad (2)$$

Measurement of equilibrium volume of distribution (V_{eq})

The direct approach to the determination of V_{eq} is to give a constant IV infusion for a period long enough to establish a steady state plasma concentration (C_{eq}). For solutes in which the systemic clearance results only from renal clearance, the peripheral (tissue) and central concentrations must be in equilibrium at this steady state and V_{eq} is defined by:

$$V_{eq} = A_{tot} / C_{eq} \quad (3)$$

where A_{tot} is the total amount of solute present. For the special case where there is no metabolism and renal clearance in the only excretion route, A_{tot} can be determined by quantitative urine collection after stopping the infusion. If the clearance is from just the central compartment (e.g. renal excretion) V_{eq} (also referred to as V_{drug}) is equal to V_{ss} [10].

The value of V_{eq} can also be estimated for subjects in renal failure that have a very low rate of renal clearance. As shown in Appendix I, for the case where the clearance is very small compared to the rate of exchange between compartments, V_{eq} is approximately equal to V_{dext} (using the notation of Wagner [11]):

$$V_{eq} \cong V_{dext} = D / B_\beta \quad (4)$$

where B_β is the coefficient of the slow, terminal exponential term of the bolus response function (eq. (1)) and D is the bolus dose. The value of B_β was determined using the deconvolution feature in PKQuest to find the 2-exponential response function.

PBPK model for extracellular solutes

A new PBPK model was developed that was consistent with the experimental data in Tables 1,2,3,4,5. Table 6

Table 1: Steady-state Volume of Distribution relative to body weight (V_{SS}) and total body water (V_{SSW}) for selected solutes.

Solute	Reference	Fraction Bound	V_{SS} (liters/Kg)		V_{SSW} (liters/liter)	Comments
			2-expon	3-expon		
Mannitol	[58]	≈ 0	.28		.48	N = 7, 28 years, 70.9 Kg, 178 cm.
EDTA		≈ 0	.265		.45	
Mannitol	[57]	≈ 0	.33	.33	.56	N = 1, 71.6 Kg, 172 cm.
amoxicillin	[62]	.17 – .23	.262	.275	.44	N = 9, 66.4 Kg
	[61]		.267	.253	.45	N = 9, 74.7 Kg, 180 cm
morphine-6-glucuronide	[59]	0–.1	.247	.245	.42	N = 20, 74.2 Kg
	[42]		.30	.40	.50	N = 10, 71 Kg
morphine-3-glucuronide	[60]		.275	.273	.47	N = 3, Dose/Kg
inulin	[37]	≈ 0	.133	.131	.22	N = 1, 87.3 Kg, 173 cm
	[39]	≈ 0	.131	.136	.23	N = 1 77.1 Kg 186 cm
	[40]	≈ 0	.20	.277	.34	N = 27 Non-linear.

Table 2: Equilibrium Volume of Distribution in Humans relative to body weight (V_{EQ}) for selected solutes.

Solute	Reference	Fast time constant (minutes)	Slow time constant (minutes)	V_{EQ} (liters/Kg)	Comments
Amoxicillin	[46]	9.8	909	0.26	N = 4, 53 Kg, 45 years Renal failure: Clearance < 10 ml/min/1.73 m^2
Morphine-6-glucuronide	[47]	23	2083	0.24	N = 6, 73.7 Kg, 48.7 years Renal Failure: Ave. clearance = 10 ml/min
Inulin	[44]	NA	NA	0.15	N = 3, Constant infusion. Normal Males, ages 21–29.
Sucrose	[45]	NA	NA	0.159	N = 3, Constant infusion.
Inulin		NA	NA	0.162	

Table 3: Steady state volume of distribution (V_{SS}) and interstitial volume (V_I) relative to body weight for β-lactam antibiotics as a function of degree of protein binding.

Solute	Reference	Fraction Bound	V_{SS} (liters/Kg)	V_I (liters/Kg)
amoxicillin	[62]	.17–.23	.26	.22
	[61]		.267	.23
piperacillin	[30]	.48	.23	.19
cefatrizine	[31]	.62	.194	.155
ceforanide	[32]	.82	.161	.12
dicloxacilllin	[63]	.97	.091	.053
amoxicillin	[29]	.17–.23	.33	.29
flucloxacillin		.93	.15	.11

summarizes the new set of PBPK parameters for the "standardhuman" with a total weight of 70 Kg and a 20% fat content. The parameters are scaled for different body weight and fat content [7]. The major difference between this parameter set and that used previously [7] is the distribution of the extracellular water (ecf_water) among the different organs. The column labeled ecf_fract is the fraction of the extravascular organ water that is extracellular-i.e. interstitial. The "adipose" ecf_fract is 1 because it is assumed that all adipose tissue water is extracellular and the cells are pure lipid. The brain ecf_fract is zero because the blood brain barrier will prevent the distribution into

the interstitial space of any of the test solutes used in Table 1. The term "solid" refers to the non-fat, organ solids It is assumed that the entire animal's fat is in the single "lipid" organ and that this organ is 80% fat. This is a major over-simplification since adipose blood flow may show large variations in different adipose tissues [12] and two different "fat" compartments have been used in some PBPK models [13]. An attempt has been made to minimize the number of adjustable parameters and a single fat compartment has provided satisfactory fits to the solutes previously investigated with PKQuest, including the highly fat soluble volatile anesthetics [5]. "Portal" refers to the organs drained by the portal vein (stomach, small and large intestine, pancreas and spleen). "Bone" refers to the inert solid component of bone that has no volume of distribution or blood flow. The blood flow and water component of the skeleton is distributed among the rest of the organs.

The organ weights in Table 6 are close to the values in the Report on the Task Group on Reference Man [12]. The "skin" is the sum of the weight of the dermis and epidermis. The organ "other" represents primarily the loose connective tissue and the organ "tendon" represents the denser connective tissue components. The total body water is 41.84 liters, in agreement with the results of Chumlea et. al. [14]. It is assumed in Table 6 that the "blood" volume includes the intra-organ blood volume, so that the organ parameters refer to the extravascular composition.

Although the blood flows to the different organs in Table 6 are in general agreement with the "proposed reference" values of Williams and Leggett [15], they have been fine-tuned in order to optimize the PBPK model predictions for selected solutes. The resting muscle blood flow was adjusted to a value of 2.25 ml/min/100 g (0.0225 L/Kg/min) to fit the D_2O data of Schloerb et. al. [16] as described previously [6]. This value for muscle blood flow is similar to the recent measurements in man of resting muscle blood flow of 2.3 [17] and 3.12 ml/min/100 gm [Ruotsalainen, #239] using [^{15}O]H_2O PET scans and of 2.5 ml/min/100 gm [18] using plethysmographic measurements of calf blood flow. This value is somewhat higher then ^{133}Xe measurements, which vary from 1.4 to 1.9 ml/min/100 gm [19]. Similarly, the adipose blood flow in Table 6 was adjusted [5] to a value of 4.4 ml/min/100 gm to fit the enflurane data of Munson et. al. [20]. This value is close to the recent human [^{15}O] H_2O measurements of subcutaneous abdominal (4.8 ml/min/100 gm), visceral (5.9) and perirenal (4.9) fat blood flow [21]. The "tendon" (e.g. connective tissue) blood flow is poorly characterized and has a large variation. The value of 1 ml/100 gm/min is representative of direct measurements of tendon blood flow using microspheres [22,23]. The total cardiac output of 5.62 L/min is close to the value of 5.82 L/min in normal young men reported by Grimby et. al. [24].

The volume of distribution in the different organs for solutes that bind to albumin is characterized by the parameter K_A^i, the ratio of the albumin concentration in the EDTA interstitial space to the plasma albumin concentration for organ i (see Appendix, II and III). The PBPK values of K_A^i for the different organs are listed in Table 6. In the analysis of the pharmacokinetics of the protein bound β-lactam antibiotics, an average value of K_A (see eq. (10)) for the entire human is estimated. This corresponds to the organ-weighted sum:

$$K_A = \sum_i ecf_i K_A^i \Big/ \sum_i ecf_i \qquad (5)$$

where ecf_i is the interstitial volume of organ i. The PBPK organ weighted values are listed in the last column of Table 6, and correspond to an average value of K_A of 4.94/17.45 = 0.28. This is identical to the value that was estimated using the β-lactam antibiotics (see fig. 15).

As described previously [4], capillary permeability limited solutes are characterized by the organ parameter fclear [i], the fraction of solute that equilibrates with the tissue in one pass through the capillary. The fclear of organ i is related to the capillary permeability-surface area product (PS_i) by the relation:

$$fclear\,[i] = 1 - \exp\left(-f_P PS_i / F_i\right) \qquad (6)$$

where f_P is the fraction free in the plasma and F_i is the organ plasma volume flow (liters/min/Kg) [7]. The parameter fclear ranges from 0 (impermeable capillary) to 1 (flow limited). In PKQuest, the default procedure is to input just one parameter, the fclear [muscle], and the permeability of all the other organs are then automatically determined using the default values of PS_i/PS_{muscle} programmed into PKQuest. This accounts for the other physiological factors that determine fclear (organ plasma flow and plasma protein binding). The following set of default PS values are assumed: liver, kidney and portal organs are flow limited, heart and lung have a PS 50 times that of skeletal muscle, brain has a PS = 0 for solutes that have fclear [muscle]<1 due to the blood brain barrier, and the rest of the organs have a PS equal to that of muscle [25]. As can be seen from eq. (6), solutes that have a high intrinsic capillary permeability (PS) can have a functional capillary permeability limitation (fclear < 1) if there is a high degree of plasma protein binding (i.e. f_P is small). This dependence of fclear on protein binding is applied

Table 4: Interstitial volume (V_I) – fraction of total extravascular water

Species	Solute	Reference	Organ	V_I	Comments
Rat	EDTA	[35,64,65]	sk. mus.	.081–091	Renal ligature-sampled 30 minutes after death.
			skin	.55–.73	
			tendon	.83	
			intestine	.28–.32	
		[66]	sk. mus	.12	Renal ligature-samples from live rat.
			skin	.63	
		[67][1]	sk. mus.	.075	Constant infusion. Measured time course of tissue uptake.
			skin	.52	
			intestine	.15–.25	Muscle, stomach and intestine equilibrated in <40 minutes.
			stomach	.23	
			adipose	.49	
			liver	.34	
			lung	.2	
			brain	≈ 0	
		[50]	skin	.61	Renal ligature – divided skin into dermis and sub-cutaneous samples.
			dermis	.67	
			subcutis	.51	
		[68][1]	sk. mus	.15	Constant infusion. Volume increased with time for skin and colon. Range indicates volume at 60 to 120 minutes
			skin	.44–.63	
			sm. intestine	.29	
			colon	.3–.41	
			adipose	1.0	
	Sulfate	[69][1]	skin	.65	Nephrectomized
			muscle	.26	
	Mannitol		skin	.66	
			muscle	.26	
	Sulfate	[70][1,2]	muscle	.12	Nephrectomized
	Inulin	[9]	sk. mus.	.12	Constant infusion.
			skin	.3	
			intestine	.12	
			liver	.2	
			lung	.27	
		[71][1]	sk. mus.	.1	Constant infusion. Tissue uptake corresponds to capillary PS ≈ 0.6 ml/min/100 gm
Rabbit	EDTA	[72]	sk. mus	.077	Renal ligature.
			skin	.42	
	EDTA	[73][1,2]	sk. mus.	.10	Renal ligature. Measured time course of tissue uptake.
			heart	.25	
	Sucrose		sk. mus.	.11	Equilibrated in < 30 minutes.
			heart	.25	
	Inulin		sk. mus.	.1	
			heart	.24	
		[74]	sk. mus.	.09	Renal ligature. Determined time constant T≈ 9 min.
			heart	.28	T ≈ 1 min.
			intestine	.2	T ≈ 1.5 min
			ear	.5	T ≈ 12 min
Cat	EDTA	[75]	sk. mus.	.13	Renal ligature.
			skin	.88	
Dog	EDTA	[76]	sk. mus.	.16	Renal ligature.
			skin	.78	

Table 4: Interstitial volume (V_I) – fraction of total extravascular water *(Continued)*

	Sulfate	[70][1,2]	muscle	.20	Constant infusion. Equilibration time <30 minutes.
	Sucrose	[49][1]	sk. mus.	.23	Constant infusion. Cannulated prepopliteal lymphatic and measured lymph sucrose
			skin	.53	
			tendon	.67	
	Thiosulfate	[51][2]	muscle	.13	Renal ligature. Equilibration time < 180 min.
			skin	.77	Equilibration time < 180 min
			tendon	.75	Equilibration time ≥ 360 min.
	Inulin		muscle	.1	Equilibration time < 180 min.
			skin	.48	Equilibration time < 180 min
			tendon	.26	Equilibration time ≥ 360 min.
Man	Inulin[1,2]	[77]	sk. mus.	.08–.11	Bolus plus constant infusion. Tissue biopsy after 20 – 120 minutes.

[1]Assumed total organ water (ml/100 gm) of: skeletal muscle, 75; heart, 78; skin, 60; subcutaneous tendon/ear, 60; stomach, 75; intestine, 73; adipose, 18.3; liver, 70; lung, 79 [35,78]. [2]Assumed plasma volume (ml/100 gm) of: skeletal muscle, 0.4; heart muscle, 2.0; skin 0.6 [64,78].

Table 5: Interstitial albumin volume as fraction of interstitial EDTA volume (V_I^A/V_I^E); the interstitial albumin concentration relative to plasma albumin (C_I/C_P); and the product $K_A = (V_I^A/V_I^E)(C_I/C_P)$.

Species	Reference	Organ	C_I/C_P	V_I^A/V_I^E	K_A	Comments
Rat	[64]	sk. mus.	0.8	0.73	0.58	Constant infusion of I^{125} rat serum albumin. Wick tissue albumin
		skin	0.69	0.6	0.4	
		tendon	0.61	0.45	0.27	
	[50]	skin-dermis	0.72	0.44	0.32	
		skin-subcut	0.72	0.57	0.41	
Rabbit	[79]	sk. mus.	0.76	0.53	0.4	Lymph albumin
		skin.	0.49	0.47	0.23	

Table 6: Spreadsheat description of PBPK parameters for the 70 Kg, 20% fat "standardhuman".

Organ	Weight (Kg)	Lipid Fraction	Solid Fraction	Solid (Kg)	ecf Fraction	water (L)	water /Kg	ecf water(L)	flow (L/Kg)	flow (L/min)	Ka	Ka*ecf
Blood	5.5	0	0.18	0.99	0.595	4.51	0.82	2.68345				
liver	1.8	0	0.3	0.54	0.23	1.26	0.7	0.2898	0.25	0.45	0.5	0.1449
portal	1.5	0	0.22	0.33	0.3	1.17	0.78	0.351	0.75	1.125	0.35	0.1228
muscle	26	0	0.22	5.72	0.15	20.28	0.78	3.042	0.0225	0.585	0.5	1.521
kidney	0.31	0	0.2	0.062	0.165	0.248	0.8	0.04092	4	1.24	0.35	0.0143
brain	1.4	0	0.2	0.28	0	1.12	0.8	0	0.56	0.784	0.1	0
heart	0.33	0	0.2	0.066	0.25	0.264	0.8	0.066	0.8	0.264	0.5	0.033
lung	0.536	0	0.2	0.107	0.2	0.428	0.8	0.08576	10.482	5.6184	0.35	0.03
skin	2.6	0	0.3	0.78	0.6	1.82	0.7	1.092	0.1	0.26	0.25	0.273
tendon	3	0	0.15	0.45	1	2.55	0.85	2.55	0.01	0.03	0.25	0.6375
other	5.524	0	0.15	0.828	0.8	4.695	0.85	3.75632	0.02	0.1104	0.25	0.9390
bone	4	0	1	4	0.5	0	0	0		0	0	0
adipose	17.5	0.8	0	0	1	3.5	0.2	3.5	0.044	0.77	0.35	1.225
Total	70	0.2		14.15		41.84		17.4572		5.6184		4.9406

below in the application of PKQuest to a series of β-lactam antibiotics with varying protein binding.

All the PBPK calculations use PKQuest [7]. A small modification of the earlier version of the software is required to account for the new situation where the interstitial volume of distribution of protein is less than that of EDTA (see Appendix, III). Four parameters characterize the interstitial volume of distribution for each organ i: 1) ecf [i] – the interstitial volume of EDTA as the fraction of the total organ water; 2) mecf – a multiplicative constant that scales all the values of ecf [i]; 3) frecf [i] – interstitial volume of the solute relative to that of EDTA; and 4) (for solutes that are protein bound) cProt [i], which is the PKQuest parameter corresponding to K_A^i. Standard values of ecf (Table 6), frecf (=1) and cProt (K_A^i, Table 6) are preprogrammed in PKQuest. The only parameter that needs to be input by the user is mecf. Setting mecf =1 indicates that the solute distributes in the standard ecf space. (The default value of mecf is -1, indicating that the solutes distributes in all the tissue (interstitial and intracellular) space.) The complete PBPK pharmacokinetics of each solute is characterized by a short Maple worksheet that lists the parameters that differ from the default "standardhuman" parameters. The complete worksheets for the 11 solutes are included in the additional file "PKQuest_worksheets.doc". For all of the solutes investigated in this paper, the kidney is the major excretion pathway. The renal clearance is described two different ways in these worksheets. If the clearance is close to the free plasma glomerular clearance, than the parameter "rclr" (glomerular filtration rate) is used. For solutes that are cleared both by glomerular filtration and tubular secretion, the single parameter Tclr [kidney] is used (the rate of renal clearance of the free (unbound) plasma solute).

PKQuest is used to find the values of the adjustable parameters that provide the best fit to the experimental data by minimizing the error function:

$$\text{Error Function} = \sum_i \frac{\left| model_i - data_i \right|}{data_i + noise} \quad (7)$$

The parameter "noise" adds a weighting factor that reduces the contribution of the low concentration data points. The default value for noise is 10% of the average concentration. (Optionally, PKQuest allows the choice of a mean square error term, and an arbitrary "noise" can be input).

Correction for antecubital vein sampling

Ideally, one would like to be able to sample arterial blood for the calculations of steady state volume of distribution and for PBPK model fitting. However, all of the data used in this paper was obtained by measuring the plasma concentrations in antecubital venous blood which differs from the arterial concentration due to the exchange with the tissues drained by the antecubital vein. A new feature has been added to PKQuest that allows one to directly correct for this effect in the PBPK model fitting. The tissue/flow distribution supplying the antecubital vein was established by applying PKQuest to the experimental data for a number of solutes for which simultaneous arterial and antecubital vein concentrations are available (Levitt, in preparation). This analysis indicated that antecubital vein blood represents approximately 10% muscle, 20% skin, 5% "other", 5% adipose and the rest (60%) A-V anastomoses. In PKQuest, specifying "arm" as the sample site outputs the antecubital vein concentration and uses this concentration to optimize the PBPK parameters using the PKQuest minimization routines [7]. This allows one to use antecubital vein blood samples when adjusting PBPK parameters for an arbitrary uncharacterized solute.

Figure 1 shows the results of this analysis for two of the extracellular solutes (DTPA and inulin) that were investigated to determine the organ composition of antecubital blood. The squares show the experimental measurements of the $^{99}Tc^m$-DTPA (left column) and inulin (right column) sampled simultaneously from the artery (black) and antecubital vein (red) after a bolus venous input. The lines show the PBPK model fits for the arterial (black) and antecubital vein (red) concentrations. The difference between the arterial and antecubital vein concentrations become negligible after the first 5 to 10 minutes because the antecubital vein blood is supplied primarily by high blood flow skin and A-V anastomoses in the hand [26]. For the solutes investigated in this paper, the differences between arterial and antecubital vein concentration are very small (e.g. see fig. 2) and this correction is of minor importance. It is fortunate that this is the case. Otherwise, one could not use antecubital vein data for PBPK modeling. Unless otherwise stated, all the PBPK model data shown in the figures in this paper correspond to antecubital vein blood.

Chiou [27] has emphasized that the measurement of the steady state volume of distribution (V_{ss}) using eq. 2 is dependent on the sampling site and has shown that the value of V_{ss} determined using antecubital vein blood will be greater than the true value of V_{ss} using arterial blood. This effect can be quantitated for the extracellular solutes investigated in this paper using the experimental or PBPK model data shown in figure 1. Using this data, the value of V_{ss} for the antecubital sampling site is from 4% (PBPK model) to 10% (experimental data) greater than the true arterial V_{ss}. The values of V_{ss} reported below are for the antecubital vein data. A small correction will be applied when these results are used to estimate the true extracellular volumes.

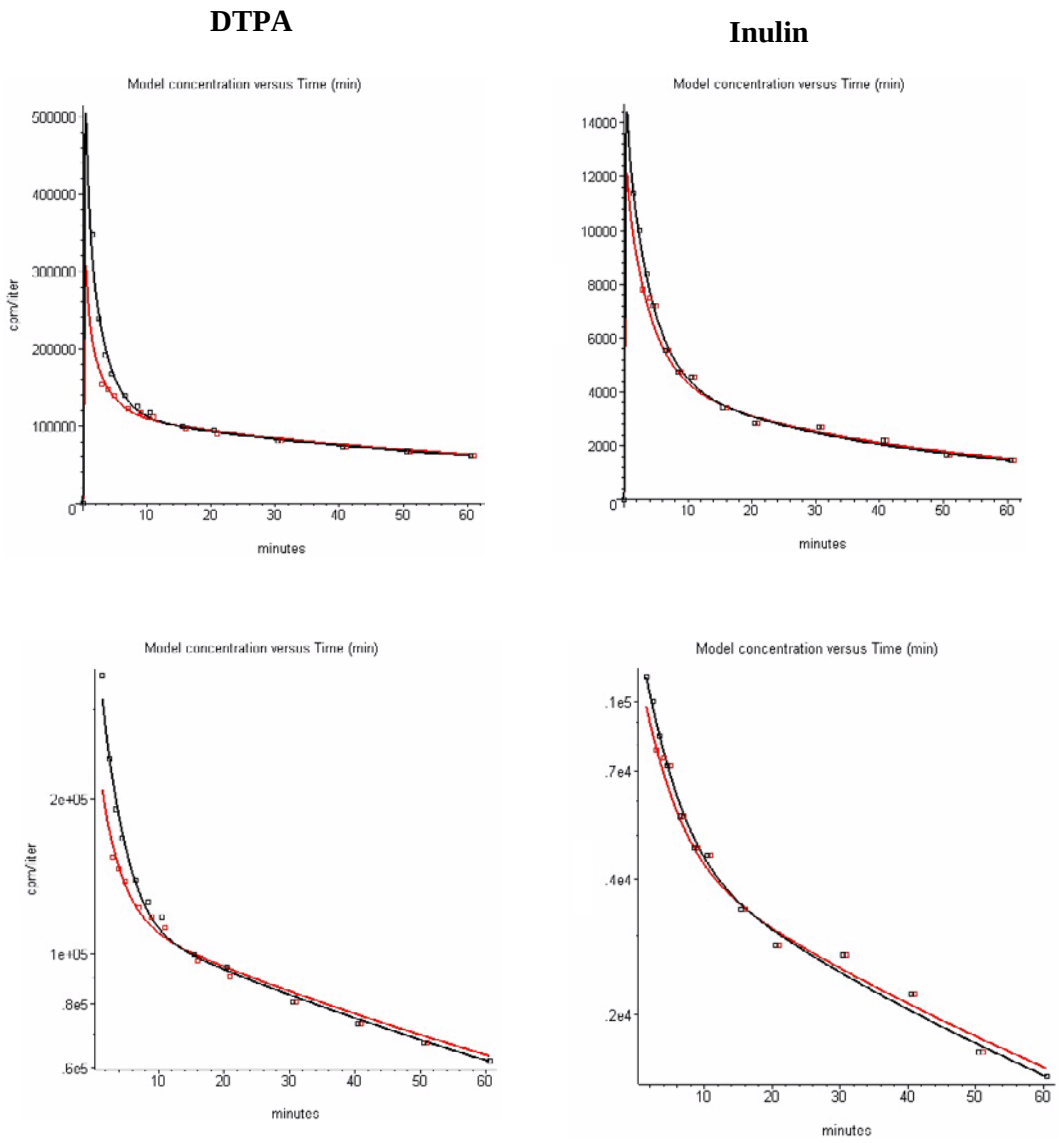

Figure 1
Arterial (black) and antecubital vein (red) concentrations of $^{99}Tc^{m}$-DTPA (right column) and inulin (left column) after a bolus injection using the experimental data (squares) of Cousins et. al. [56]. The solid lines indicate the PBPK model predictions for the arterial (black) and antecubital vein (red) concentrations. The top row shows a plot of the absolute concentration and the bottom row is a semi-log plot of the same data. The PBPK parameters for DTPA were identical to those used for EDTA (see fig. 3).

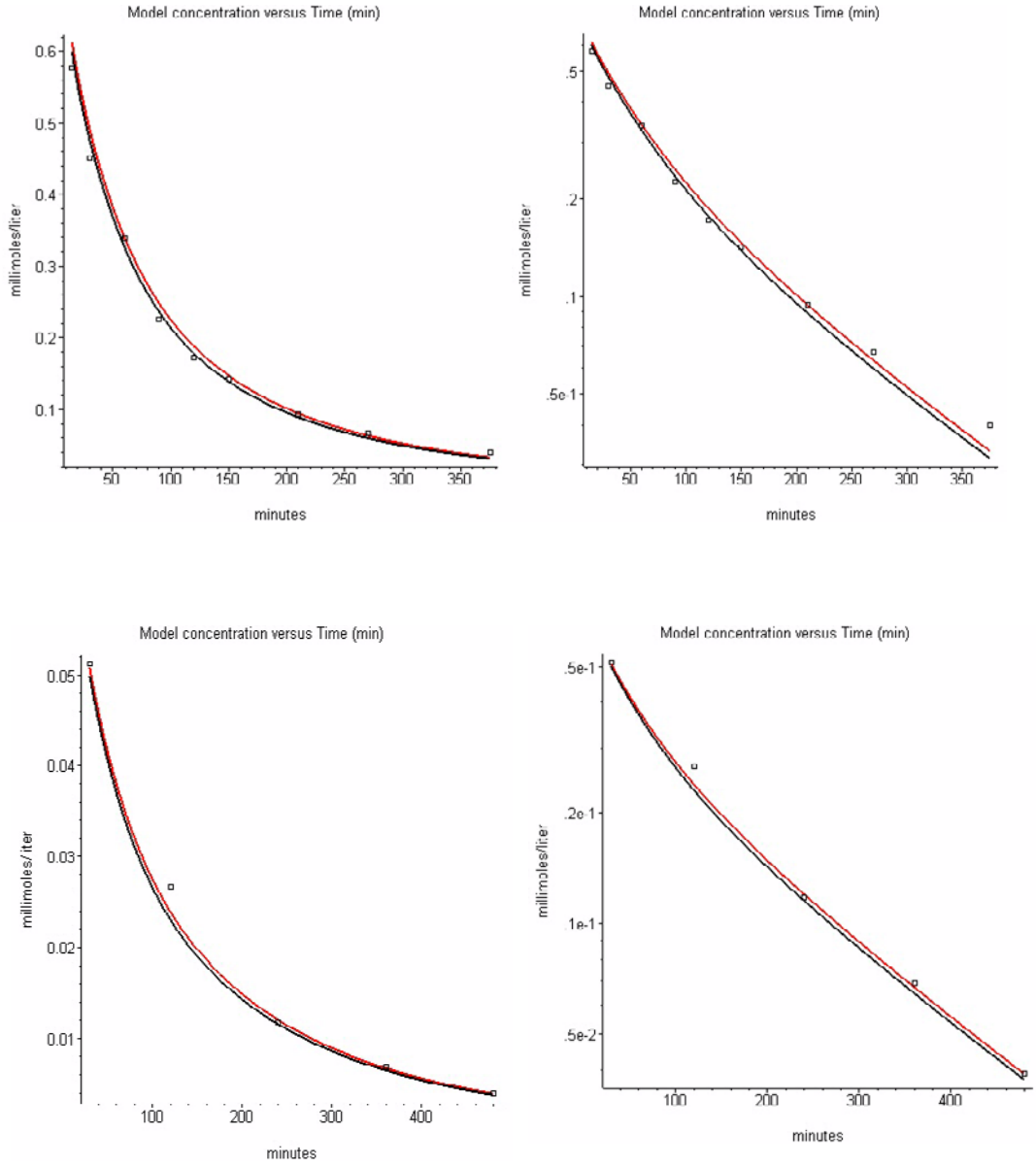

Figure 2
Comparison of PBPK model predictions and experimental data for mannitol plotted using linear (left) or semi-log (right). The predictions for the experimental data of Laker et. al. [57] (top) and Elia et. al. [58] (bottom) are shown using the parameters in Table 6. Both the model arterial (black) and antecubital vein (red) concentration curves are shown.

Results

Experimental measurements of whole animal and individual organ volumes of distribution for extracellular solutes

Table 1 summarizes the experimental measurements in humans of the steady state volume of distribution (V_{ss}) for mannitol, EDTA, amoxicillin, morphine-3-glucuronide, morphine-6-glucuronide and inulin. The volume of distribution is expressed in terms of total body weight (V_{ss}, liters/Kg) and total body water (V_{ssw}, liters/liters). The latter calculation was based on an assumption of a value of 41 liters of water for the standard 70 Kg man with 20% body fat [14]. The total body water was adjusted for body fat estimates if information was available. Table 2 lists the values of the equilibrium volume of distribution (V_{eq}) for amoxicillin, morphine-6-glucuronide, sucrose and inulin (see Methods). Table 3 lists the V_{ss} and the interstitial volume (V_I) for a series of β-lactam antibiotics with varying amounts of plasma protein binding. V_I was estimated by subtracting a plasma water volume of 2.68 liters/70 Kg from V_{ss}. The human serum protein binding values used in Tables 1,2,3 were from the following references: amoxicillin [28,29]; piperacillin [30]; cefatrizine [31]; ceforanide [32]; dicloxacillin [33]; flucloxacillin [29,33]; morphine-3-glucuronide and morphine-6-glucoronide [34]. Table 4 lists the interstitial volume as a fraction of total extravascular organ water for selected solutes in rats, rabbits, cats, dogs and man.

The solutes listed in Table 4 have a rapid, possibly flow limited, exchange between the blood and interstitial space so that the interstitial space equilibrates with the blood. In contrast, albumin has a very slow rate of tissue-plasma exchange with a time constant of about 100 hours in the rat [35]. Because of this low permeability, the steady state interstitial albumin concentration in a given tissue (C_I) is less than the plasma concentration and is determined by the balance between the rate of trans-capillary exchange and the rate of removal by lymph flow [36]. The standard procedure used to measure this concentration C_I is to sample the lymph draining that tissue, or to use the wick method to sample the free tissue albumin. The interstitial albumin volume of distribution V_I^A for that tissue is then defined by:

$$V_I^A = (Total\ Extravascular\ Albumin)/C_I \quad (8)$$

The fourth column in Table 5 lists the steady-state albumin tissue/plasma concentration ratios (C_I/C_P) and the fifth column lists the corresponding ratio V_I^A/V_I^E (where V_I^E is the interstitial volume of EDTA) for skeletal muscle, skin and tendon. V_I^A is less than V_I^E because the interstitial matrix behaves like a size exclusion gel, restricting the albumin volume of distribution [3]. This excluded volume is larger in skin and tendon then in skeletal muscle, resulting, presumably, from varying concentrations of collagen and hyaluronan in the different tissues. The sixth column is the product of these two ratios:

$$\begin{aligned} K_A^i &= (C_I/C_P)(V_I^A/V_I^E) = (C_I V_I^A/V_I^E)/C_P \\ &= (Albumin\ concentration\ in\ EDTA\ space)/C_P \end{aligned} \quad (9)$$

This product for organ i, which will be referred to as K_A^i, is the relevant parameter determining the pharmacokinetics of albumin bound solutes, such as the β-lactam antibiotics (see Appendix, II).

PBPK model for extracellular solutes

The PKQuest PBPK model [7] was applied to the extracellular solutes using the new set of parameters (Table 6). A comparison of the model predictions with the experimental data is shown in figs. 2,3,4,5 for mannitol, EDTA, morphine-6-glucuronide and morphine-3-glucuronide – solutes with low or negligible protein binding. Since one of the purposes of this analysis is to find a single, unique PBPK model applicable to all extracellular solutes, the identical set of PBPK parameters has been used in all these figures. The only parameter that was varied for each solute is the renal clearance, determined using the optimization feature in PKQuest (see Methods). Figure 2 shows the PBPK model predictions for both the arterial and antecubital vein concentration (see Methods). It can be seen that the difference is small. In all other figures, only the antecubital vein concentration is shown.

All of the solutes shown in figs. 2,3,4,5 have been assumed to be flow limited. This is clearly not the case for inulin, which is the prototypical capillary permeability limited solute. In addition, the interstitial volume of distribution of inulin (V_I) is clearly significantly smaller than that of EDTA (Table 1). In PKQuest, the parameter mecf scales the interstitial volume of all non-blood organs by the same amount. Thus, for inulin, there are 3 adjustable parameters: 1) the renal clearance ("rclr"); 2) the interstitial volume relative to that for EDTA ("mecf"); and 3) the capillary permeability for muscle ("fclear [muscle]") which sets the permeability for all the other organs (see Methods). The parameter fclear indicates the fraction of the solute that equilibrates with the tissue in one pass through the capillary. The flow-limited case corresponds to an fclear equal to 1. Figure 8 shows the PBPK model results for four different sets of experimental inulin data. The values of mecf (= 0.42) and fclear [muscle] (= 0.409, corresponding to PS_{muscle} = 0.61 ml/min/100 g, see eq. (6)) were first determined by optimizing the fit to the data of Odeh et. al. [37] (top row, fig. 6). A good fit (average error less than 2%) was obtained with the 3 adjustable parameters. To test the validity of this result, 3 other sets of experimental data were fitted, using these identical values of mecf and fclear [muscle] and only adjusting the

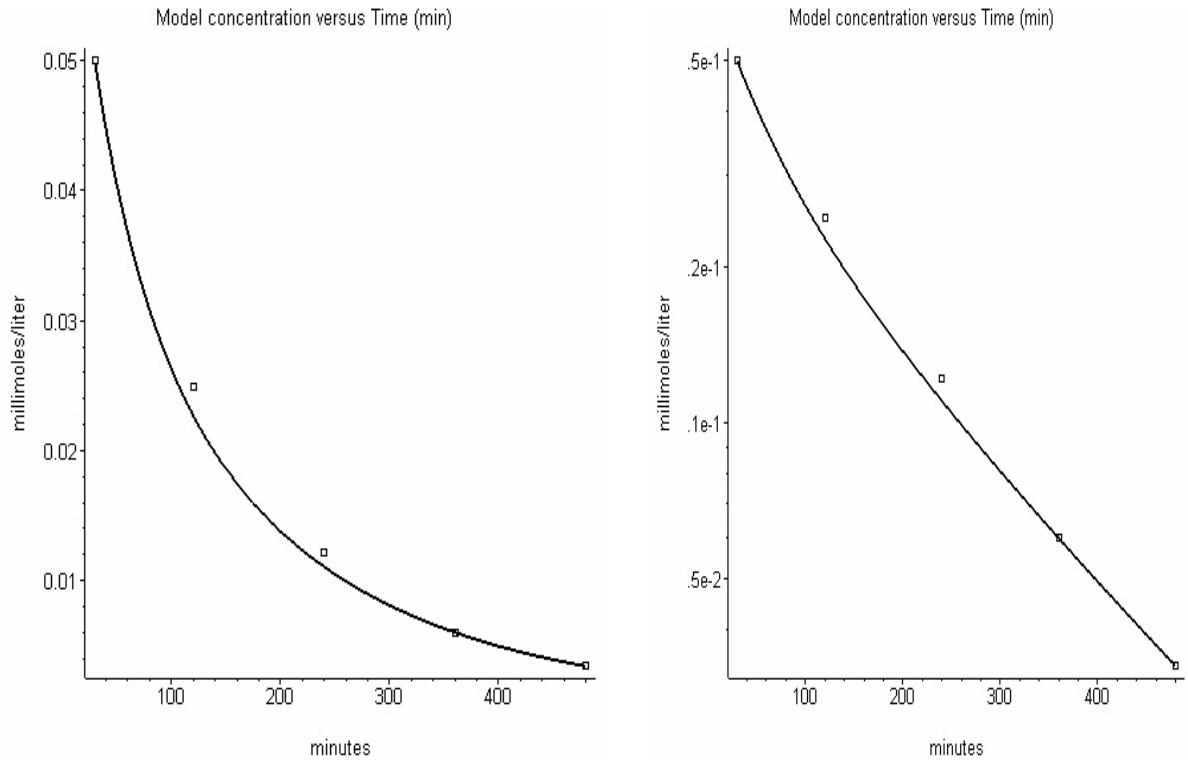

Figure 3
Comparison of antecubital PBPK model predictions (line) and experimental data (squares) for EDTA [58] plotted using linear (left) or semi-log (right).

renal clearance. The result of this procedure are shown in figure 6 for the experimental data of Orlando et. al. [38] (second row), Ladegaard-Pedersen et. al. [39] (third row) and Prescott et. al. [40] (bottom row). The agreement between the PBPK model and the experimental data is quite good, except for the long time data of Prescott et. al. [40]. This discrepancy is expected, since the inulin clearance in the experiments of Prescott et. al. was non-linear, decreasing by about 50% at low concentrations (long times). It is not clear why the data in the other three experiments in fig. 6 do not show this marked non-linearity.

Figures 7,8,9,10,11,12 compare the PBPK model predictions with experimental data for the six β-lactam antibiotics listed in Table 3 (amoxicillin, piperacillin, cefatrizine, ceforanide, flucloxacillin and dicloxacillin). The influence of the protein (albumin) binding on the pharmacokinetics of these solutes is characterized by the default PKQuest values for K_A^i in the different organs (Table 6, see Appendix, II and III) and the experimental values for the fraction bound in plasma (f_p, Table 1). The effect of including a capillary permeability limitation was investigated for these solutes because, as discussed above (see eq. (6)), one would predict that solutes with a high amount of protein binding should be capillary permeability limited. (All the other parameters were identical to those used in figs. 2,3,4,5). The addition of a capillary permeability limitation provides a significant improvement

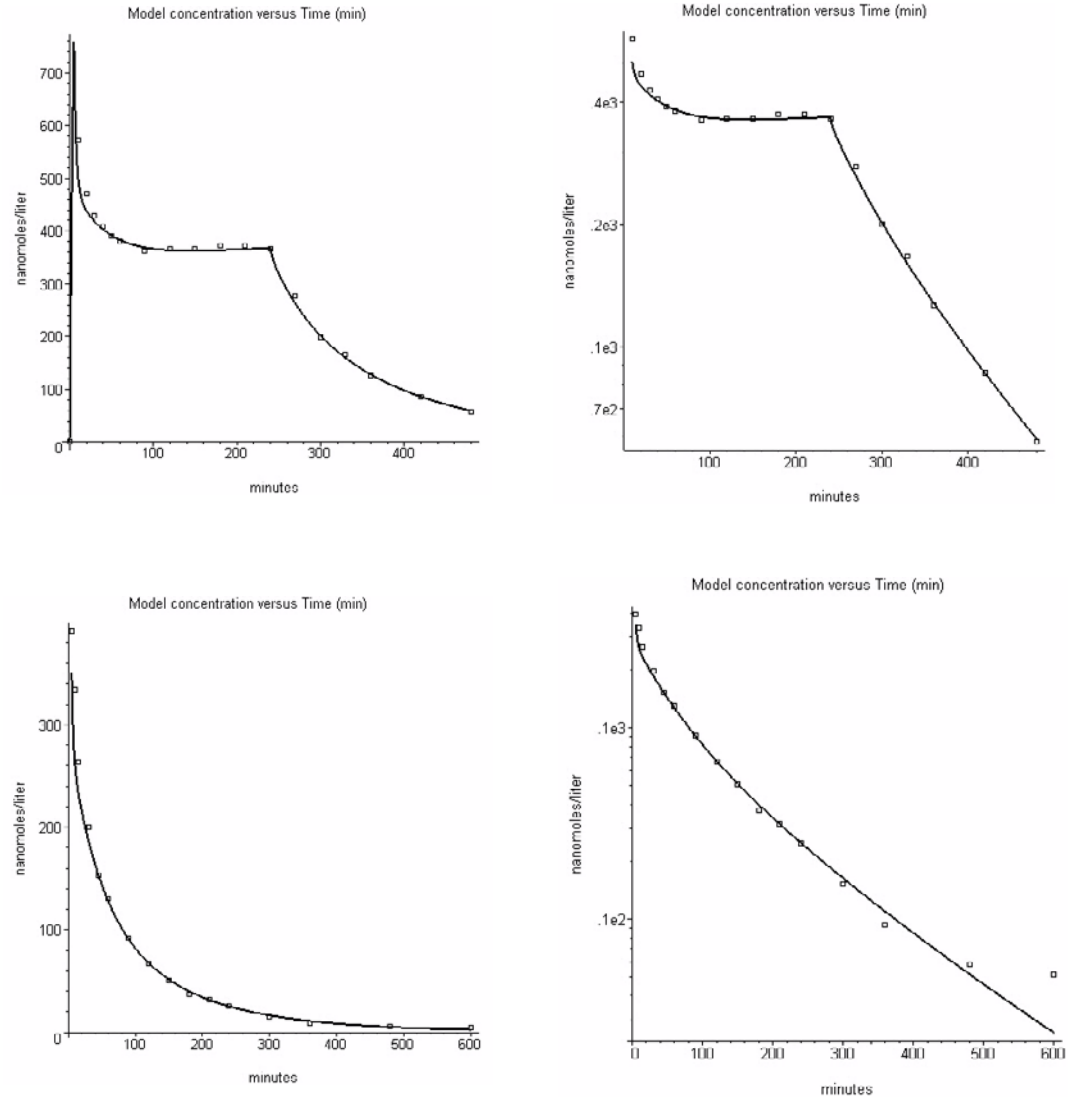

Figure 4
Comparison of PBPK linear (left) or semi-log (right) plots of model predictions and experimental data for morphine-6-glucuronide for experimental data of Lotsch et. al. [59] (top row) and Penson et. al. [42] (bottom row).

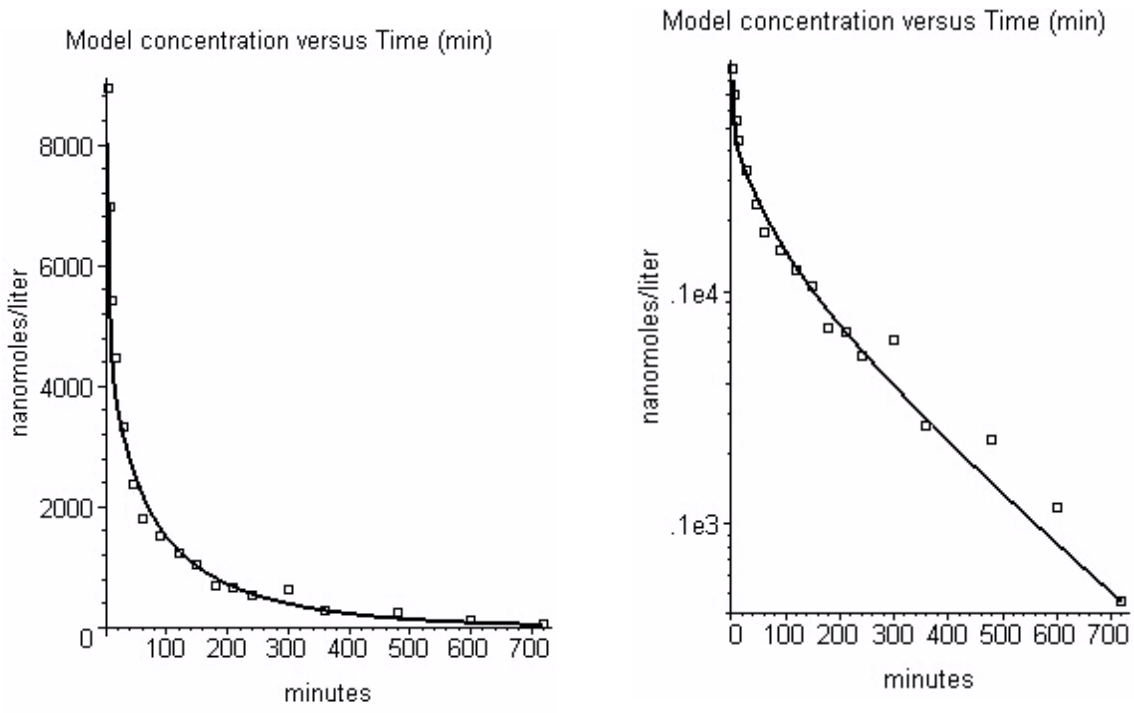

Figure 5
Comparison of PBPK linear (left) or semi-log (right) plots of model predictions and experimental data for morphine-3-glucuronide for experimental data of Penson et. al. [60].

in the fit between the PBPK model and the experimental data for the two antibiotics with the highest degree of binding, dicloxacillin (97% bound, fig. 12) and flucloxacillin (93% bound, fig. 11). For ceforanide (fig. 10), which is 82% bound, there is a slight improvement in the fit with the addition of a small permeability limitation. The value of the PS product for these three permeability limited solutes is 11.3 ml/min/100 g (fclear= 0.25) for dicloxacillin, 7.0 ml/min/100 g (fclear = 0.344) for flucloxacillin and 5 ml/min/100 g (fclear = 0.52) for ceforanide. For the other antibiotics (amoxicillin, piperacillin and cefatrizine) with protein binding of 62% or less, the addition of a capillary permeability limitation does not significantly improve the fit. For these flow limited antibiotics (amoxicillin, piperacillin, cefatrizine), there is only 1 adjustable parameter – the renal clearance. For the capillary permeability limited solutes (ceforanide, flucloxacillin, dicloxacillin) there are two adjustable parameters, the renal clearance and fclear [muscle].

This new PBPK parameter set (Table 6) also provided good fits (not shown) to the other solutes that have been previously investigated with PKQuest (propranolol [7], D_2O and ethanol [6], anesthetic gases and toluene [5]). The slightly modified Maple worksheets describing these solutes are available on the PKQuest web site http://www.pkquest.com.

Discussion

Volume of distribution of selected extracellular solutes in humans

Table 1 summarizes the experimental measurements in humans of the steady state volume of distribution (V_{ss}) for mannitol, EDTA, amoxicillin, morphine-3-glucuronide, morphine-6-glucuronide and inulin. In order to be included in this table, solutes had to meet the following criteria: 1) extracellular distribution; 2) low level of plasma protein binding, 3) no evidence of any unusual tissue binding or accumulation; 4) major excretory pathway is renal; 5) linear pharmacokinetics; and 6) published

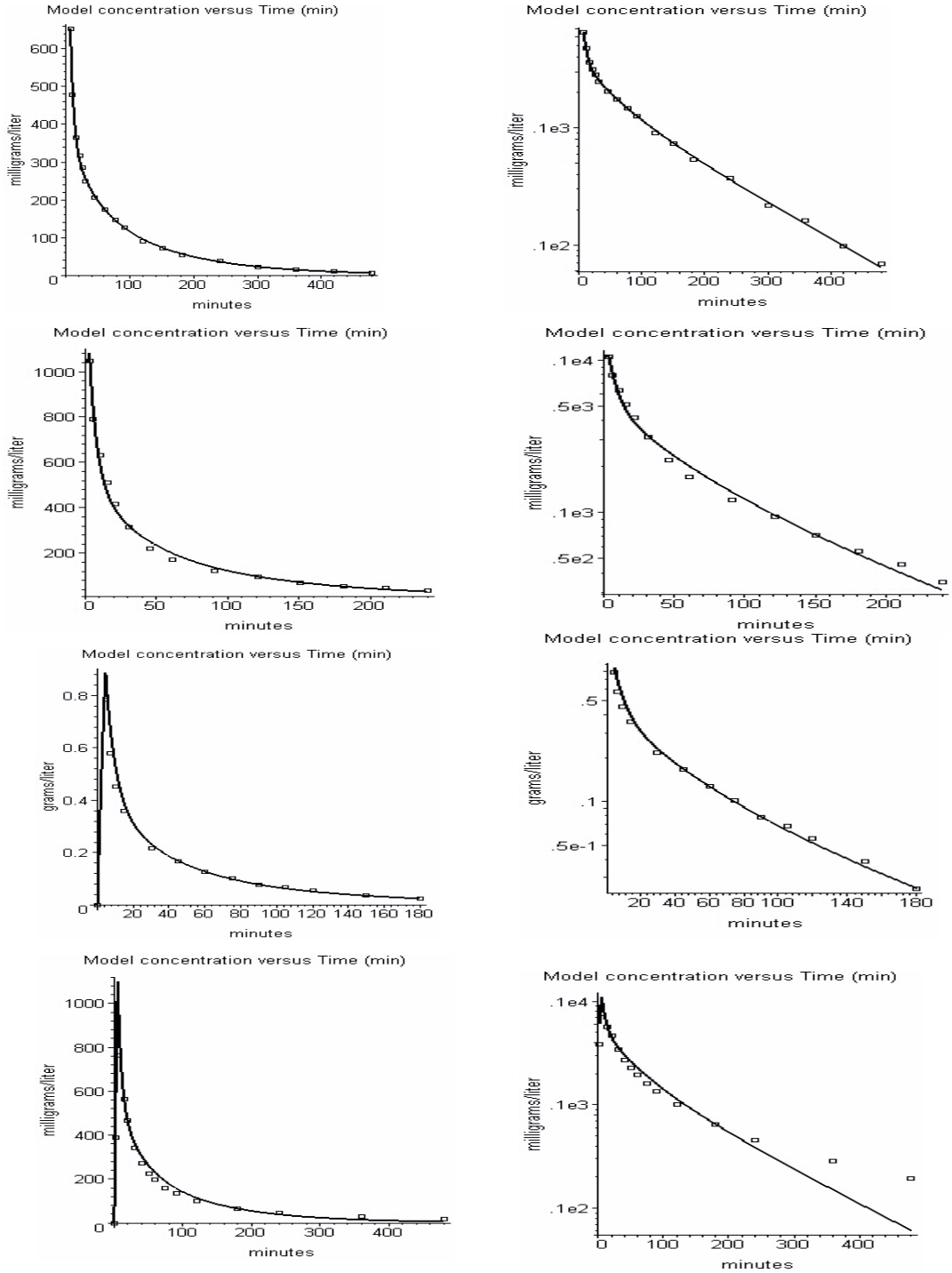

Figure 6
Comparison of PBPK linear (left) or semi-log (right) plots of model predictions and experimental data for inulin. The parameters rclr, mecf, and fclear [muscle] were adjusted to give the optimal fit to the data of Odeh et. al. [37] (top row). These values of mecf and fclear [muscle] were then used to fit the experimental data of Orlando et. al. [38] (second row), Ladegaard-Pedersen et. al. [39] (third row) and Prescott et. al. [40] (bottom row), varying only the renal clearance to obtain the best fit.

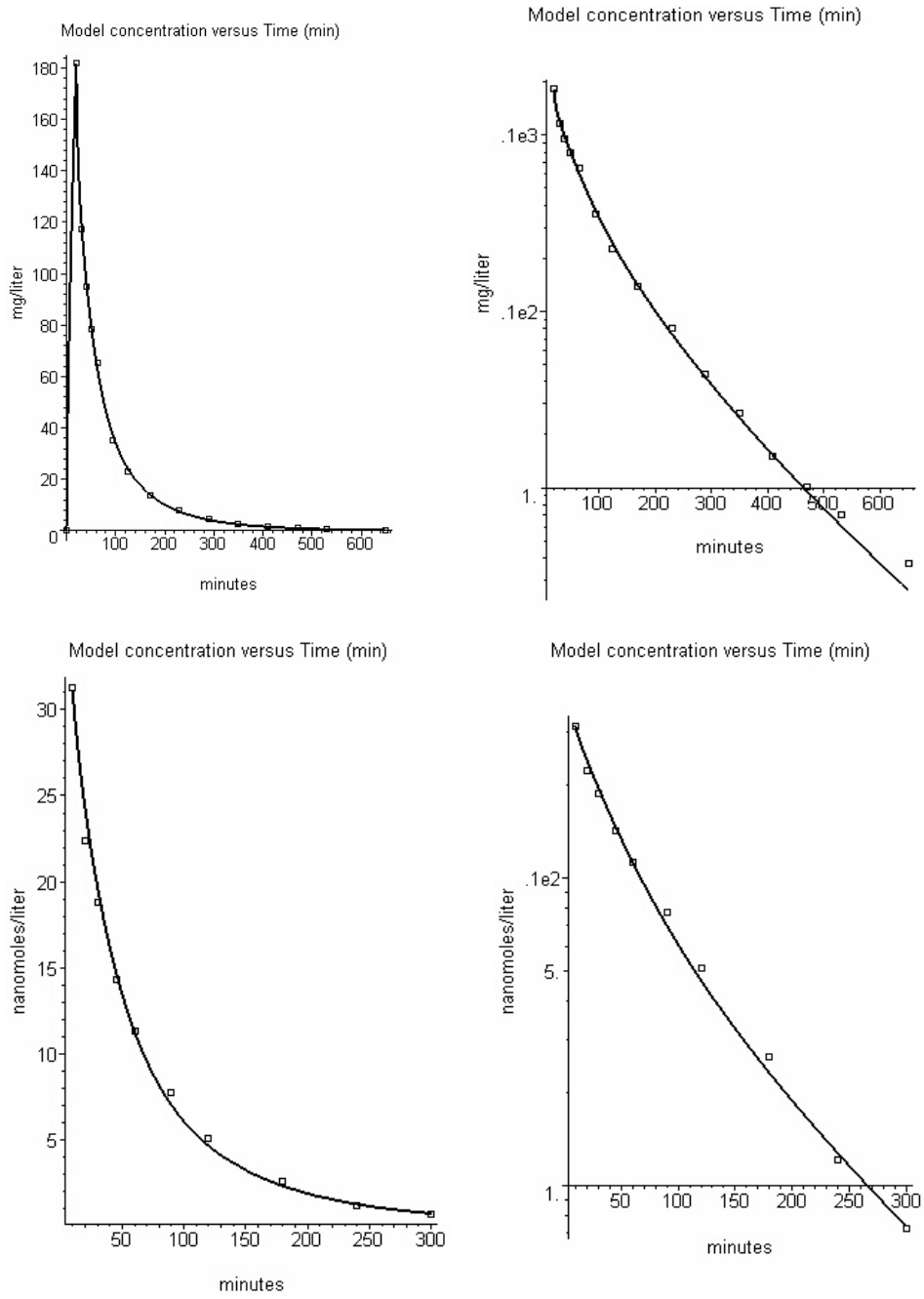

Figure 7
Comparison of PBPK linear (left) or semi-log (right) plots of model predictions and experimental data for amoxicilllin for experimental data of Sjovall et. al. [61] (top row) and Arancibia et. al. [62] (bottom row). The flow limited PBPK model is used (no capillary permeability limitation).

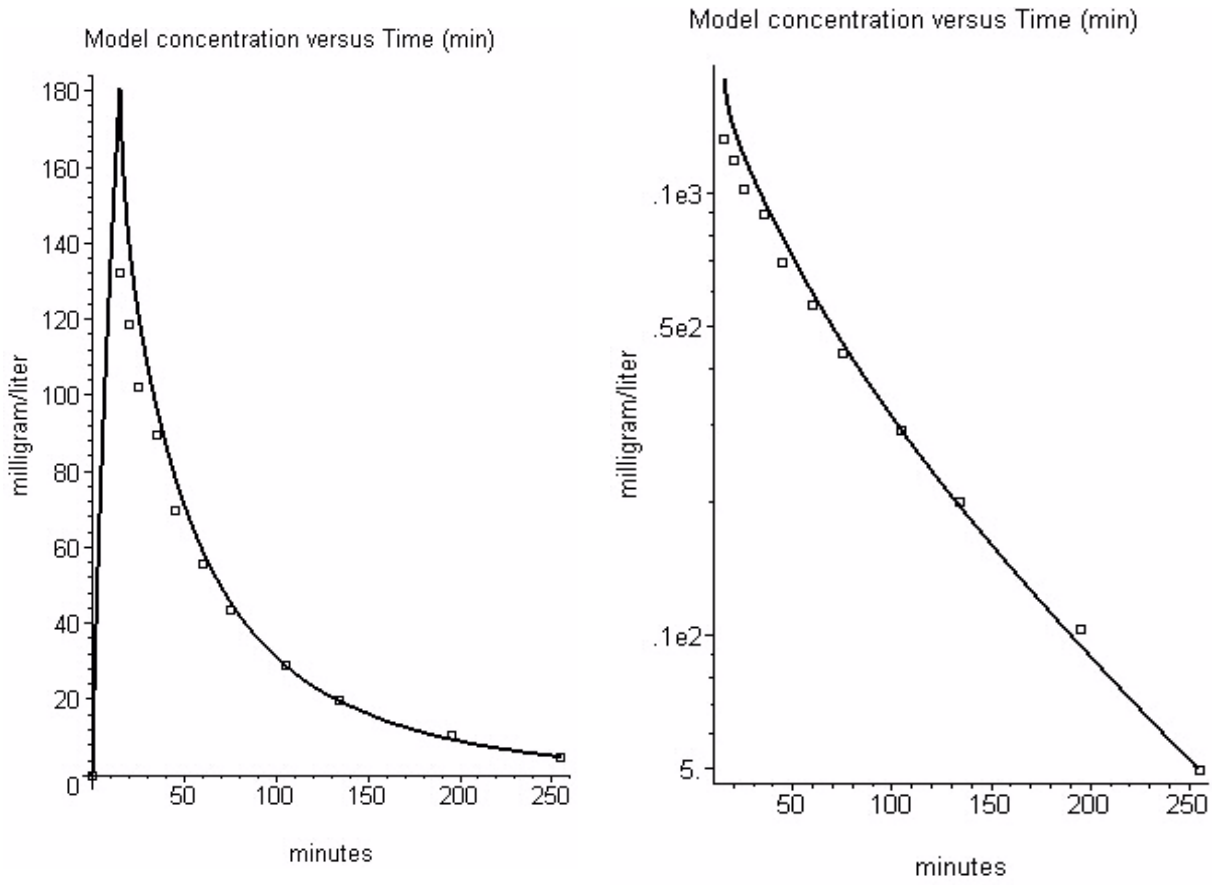

Figure 8
Comparison of PBPK linear (left) or semi-log (right) plots of model predictions and experimental data for piperacillin from Lode et. al. [30]. The flow limited PBPK model is used (no capillary permeability limitation).

data describes the plasma time course in humans in enough detail that the value of V_{ss} could be recalculated using PKQuest (see Methods). These 6 conditions are quite restrictive and most other drug classes do not meet all of these conditions. For example, although the aminoglycosides (e.g. gentamicin) satisfy conditions 1, 2, 4 and 5 and 6, they are known to be actively concentrated in the renal cortex and in several other organs [41]. There is even a suggestion that inulin, the classic extracellular solute, may not satisfy condition 5 because of non-linear renal clearance [40].

There are two ambiguities in this calculation of V_{ss}. First, as discussed above in the Methods section, the use of antecubital vein samples should lead to a value of V_{ss} that is about 5 to 10% greater than the true value. Second, the calculation of V_{ss} using eq. (2) depends on an accurate extrapolation of the venous concentration to long times to determine the integrated mean residence time. Errors in

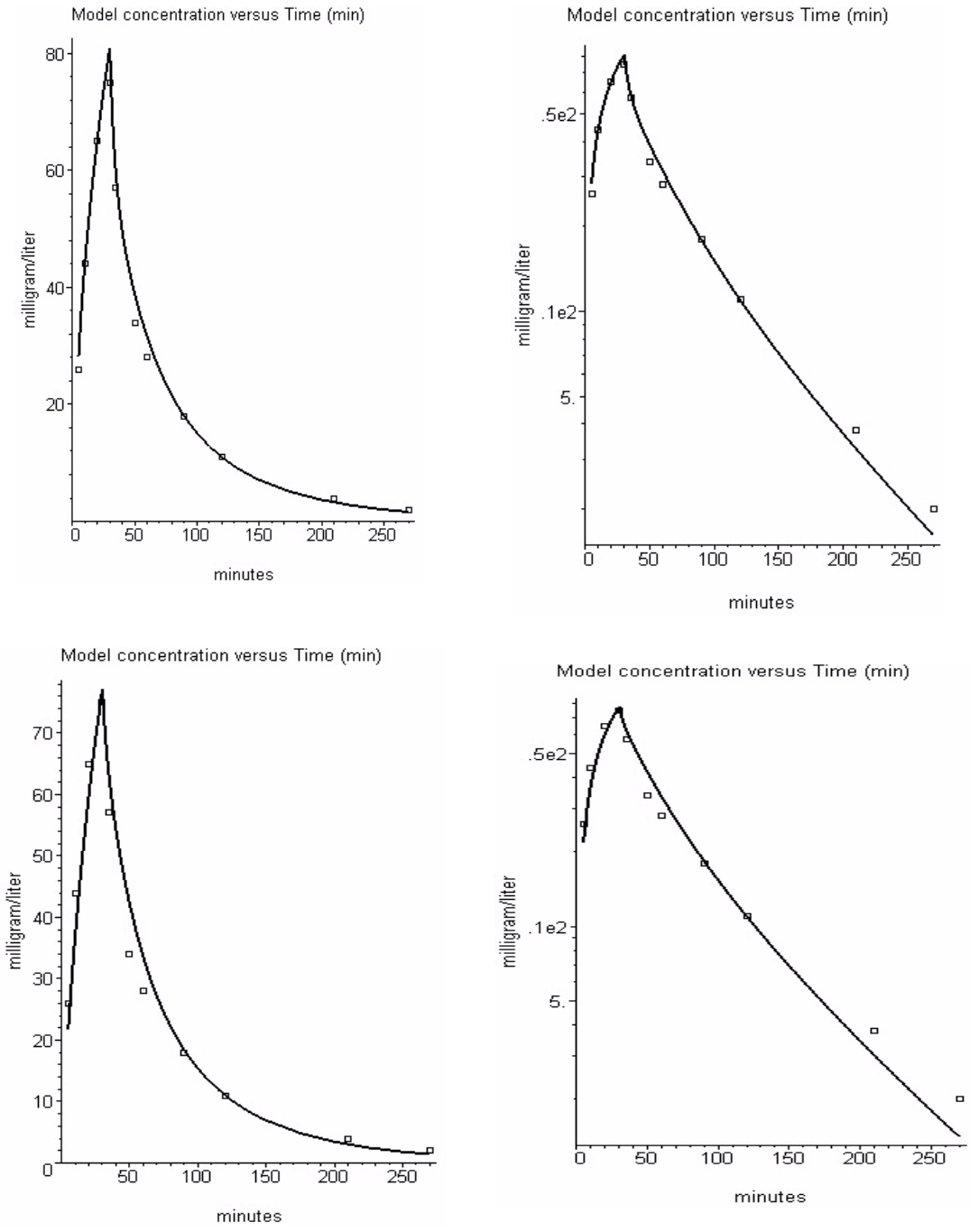

Figure 9
Comparison of PBPK linear (left) or semi-log (right) plots of model predictions and experimental data for cefatrizine from Pfeffer et. al. [31]. The top row is for the flow limited model (fclear = 1) with an average error between PBPK model and experimental data of 5.4%. The addition of a small capillary permeability limitation does not significantly improve the fit (not shown).

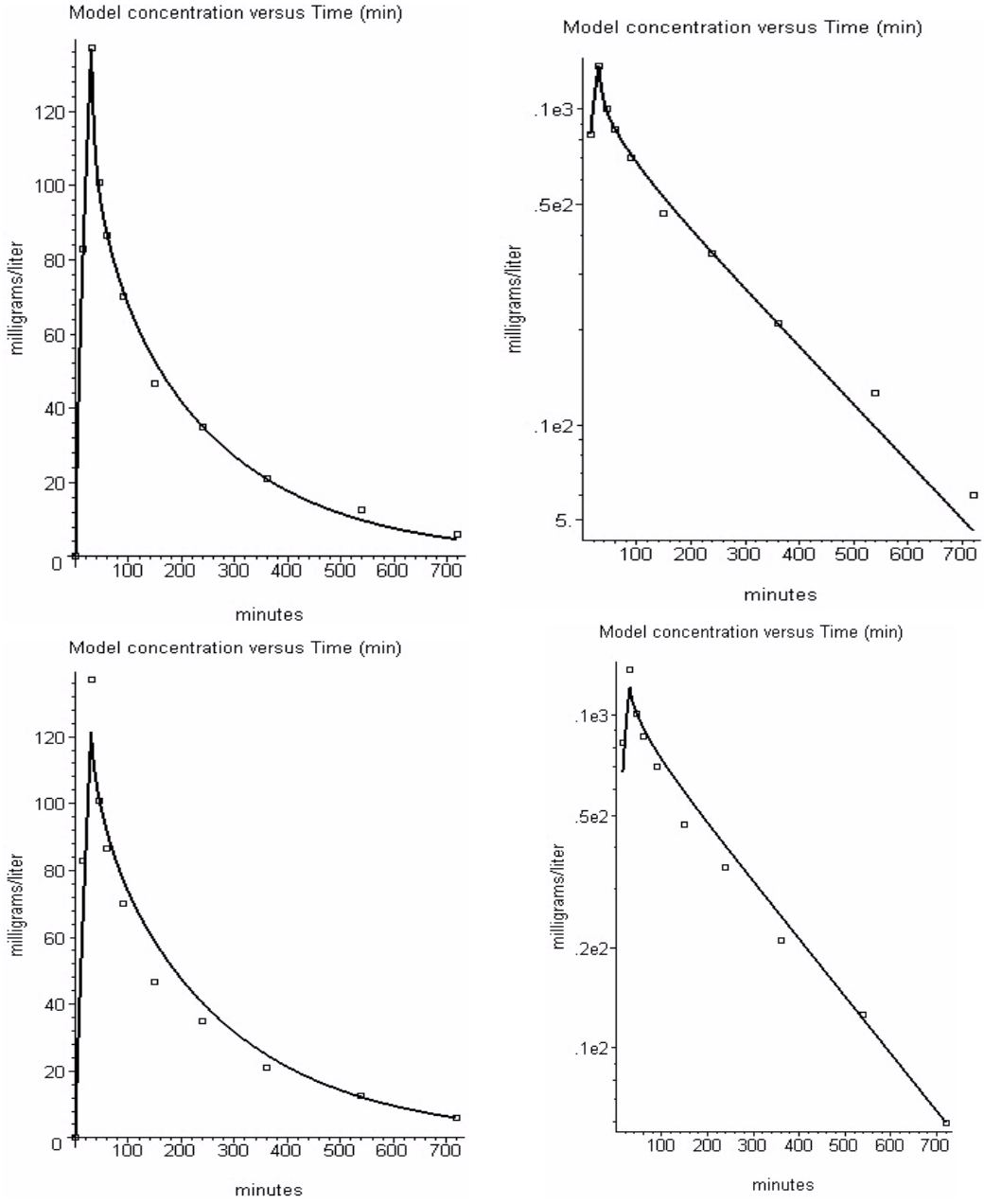

Figure 10
Comparison of PBPK linear (left) or semi-log (right) plots of model predictions and experimental data for ceforanide from Pfeffer et. al. [32]. The top row is the optimal fit for the case of a capillary permeability limitation (fclear [muscle] = 0.518, PS_{muscle} = 5 ml/min/100 gm, average error = 4.3%). The bottom row is the best fit for the flow limited case (fclear = 1, average error = 8.6%).

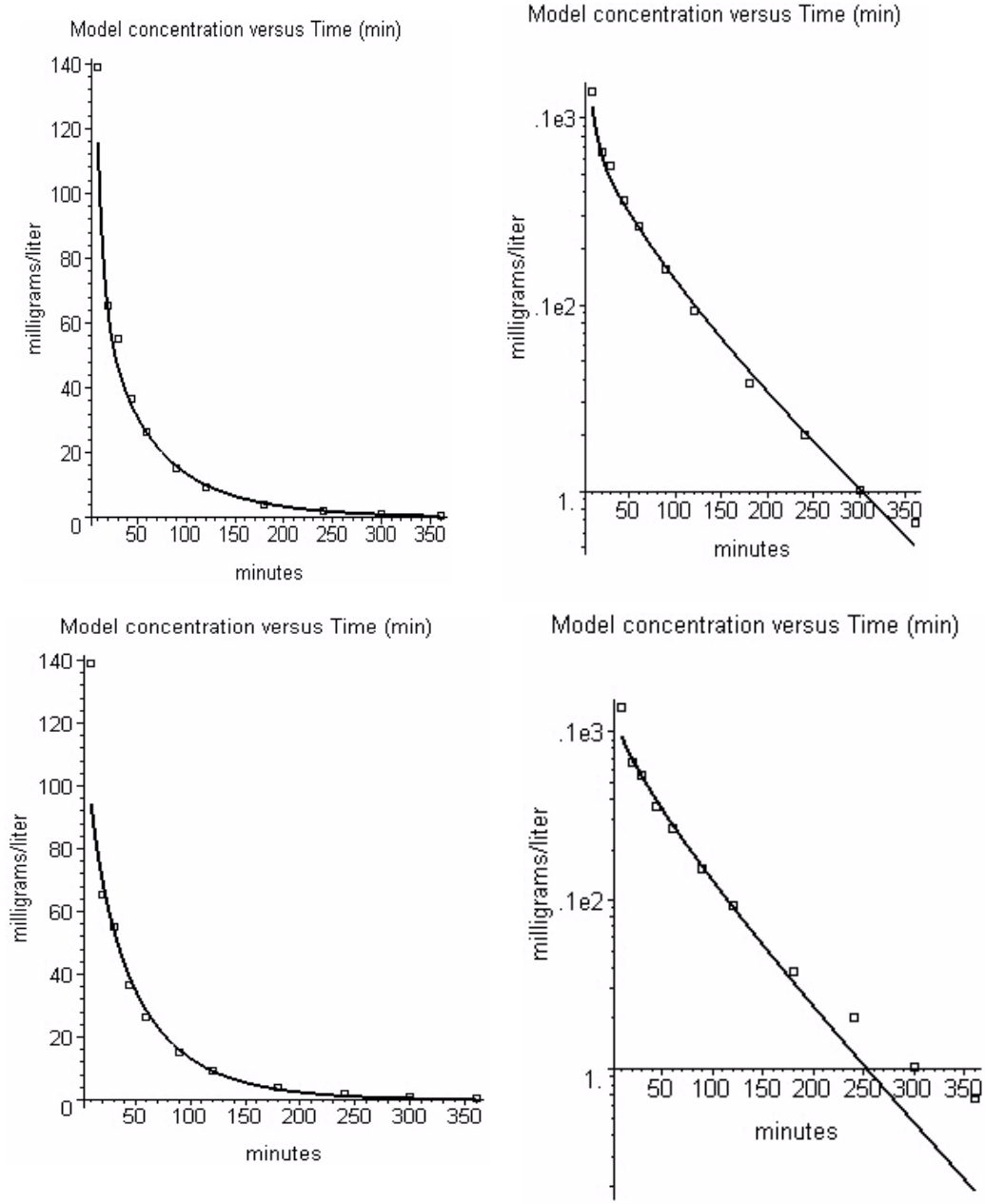

Figure 11
Comparison of PBPK linear (left) or semi-log (right) plots of model predictions and experimental data for flucloxacillin from Wise et. al.[29]. The top row is the optimal fit for the case of a capillary permeability limitation (fclear [muscle] = 0.344, PS_{muscle} = 7.0 ml/min/100 gm, average error = 6.4%). The bottom row is the best fit for the flow limited case (fclear = 1, average error = 11%).

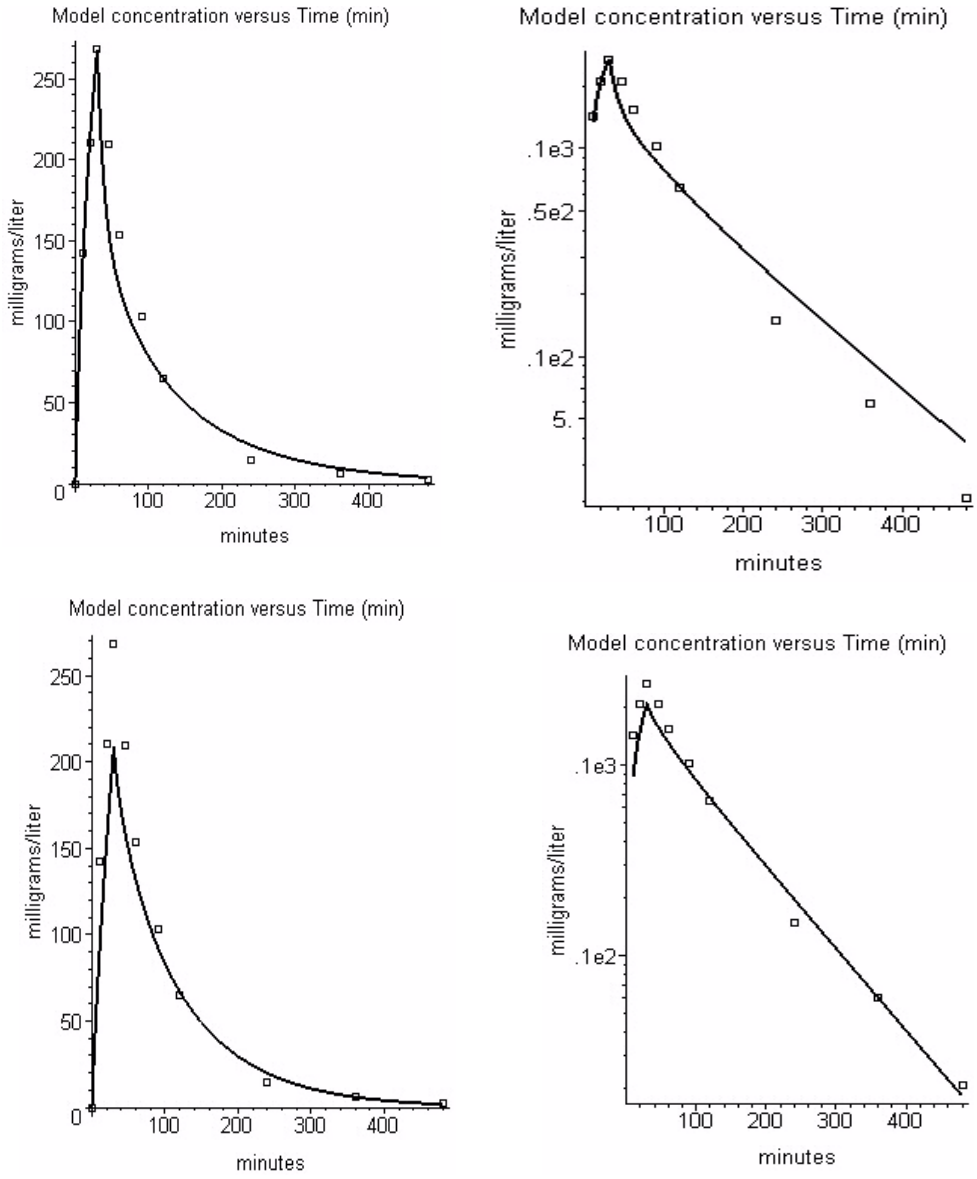

Figure 12
Comparison of PBPK linear (left) or semi-log (right) plots of model predictions and experimental data for dicloxacillin from Lofgren et. al. [63]. The top row is the optimal fit for the case of a capillary permeability limitation (fclear [muscle] = 0.25, PS_{muscle} = 11 ml/min/100 gm, average error = 12%. The bottom row is the best fit for the flow limited case (fclear = 1, average error = 18%).

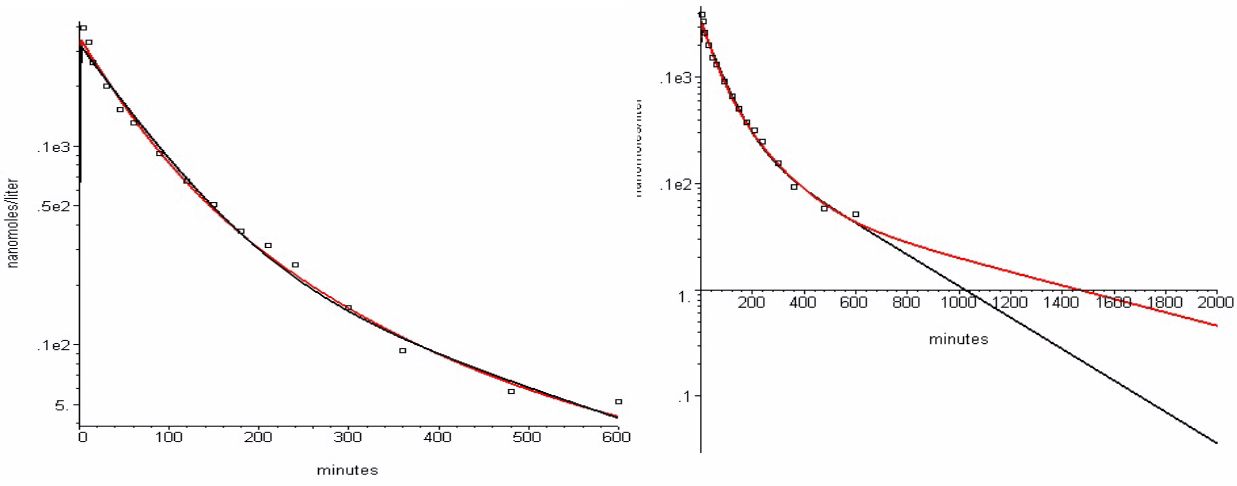

Figure 13
Comparison of morphine-6-glucuronide experimental data [42] with venous concentration predicted using either a 2 (black) or 3 (red) exponential bolus response function.

the long time, low concentration venous concentrations can produce large errors in the extrapolated MRT. The procedure used in Table 1 involves using deconvolution to find a multi-exponential unit bolus response function, and then integrating this function from 0 to infinity (see eq. 2). The values of V_{ss} were calculated using either a 2 or 3 (if there were enough experimental data points) exponential function. Some indication of the accuracy of this extrapolation can be obtained by comparing the results for the 2 and 3 exponential functions, listed in Table 1. The calculation with the largest difference between the V_{ss} calculated for the 2 and 3-exponential function is for the morphine-6-glucuronide data of Penson et. al. [42]. Figure 13 compares the semi-log fits for the 2 (black line) and 3-exponential (red line) functions to the experimental venous data. In the figure on the left, which displays the two fits over the time of the experimental measurements (600 minutes), the fits look almost identical. However, as can be seen in the right figure, which extends the fits out to 2000 minutes, the 3-exponential fit has a markedly different extrapolation, producing the 33% greater value of V_{ss} for the 3-exponential fit (Table 1). As this figure illustrate, the value of V_{ss} will be underestimated if there is a compartment with a very long time constant (e.g. 690 minutes for the 3-exponential fit, fig. 1). For each solute in Table 1, the 2-exponential fit was superior using the standard statistical tests [43], and this is the value that was used to determine V_{ssw} (Table 1) and was used in this paper.

Both of these ambiguities can be avoided if one can measure the true equilibrium volume of distribution (V_{eq}). One approach that has been used in humans is to first establish a steady state concentration using a long, constant IV infusion. The equilibrium volume of distribution (V_{eq}) is then determined using eq. 3, where C_{eq} is the steady state plasma concentration, and A_{tot} is the total amount of solute in the animal. If the solute is not metabolized and the kidney is the only route of excretion, A_{tot} can be determined by quantitative urine collection after stopping the infusion. The measurements of Schwartz et. al. [44] of the V_{eq} of inulin represent the most detailed investigation of this type in humans (Table 2). Schwartz et. al. [44] infused inulin for periods up to 30 hours and

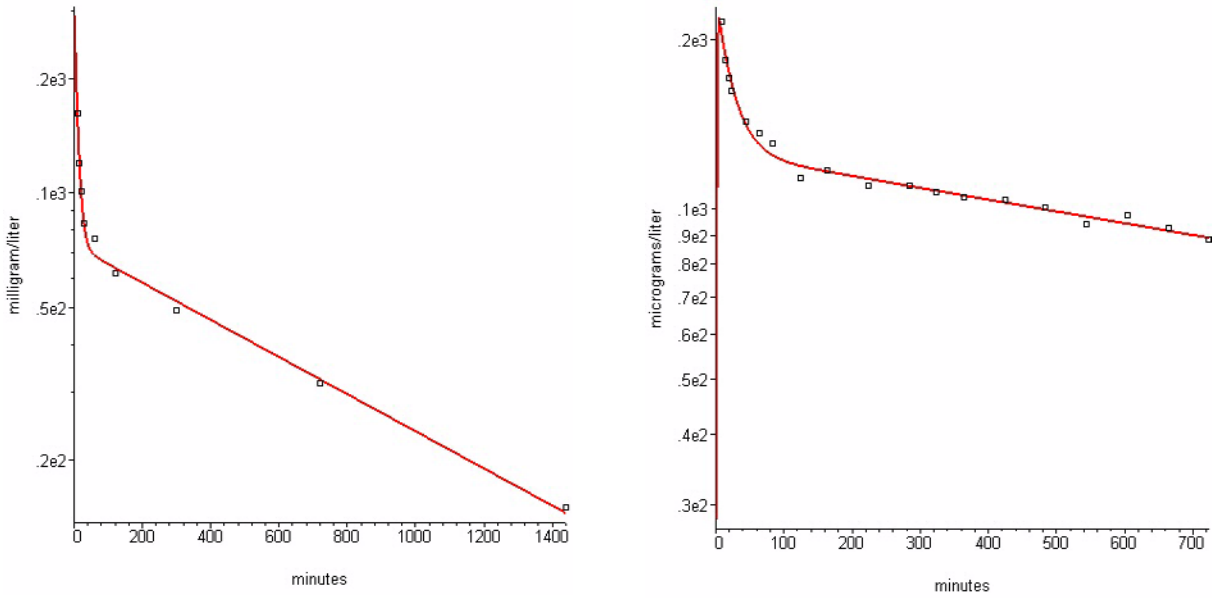

Figure 14
Comparison of experimental data with venous concentration predicted using a 2-exponential bolus response function for amoxicillin (left) and morphine-6-glucuronide (right) in subjects with renal failure.

found that equilibration was at least 95% complete by 5 hours. This indicates that there are no compartments with significant volumes of distribution with time constants longer than 300 minutes. There is some evidence that the renal clearance of inulin is non-linear [40] which, if correct, could produce an error in the V_{ss} calculation for inulin in Table 1. However, this non-linearity would have no effect on the V_{eq} calculations in Table 2. Deane et. al. [45] used this constant infusion approach to compare the V_{eq} of inulin and sucrose and reported that the sucrose V_{eq} is slightly smaller than that of inulin (Table 2). This result is not consistent with the other measurement of V_{eq} or V_{ss} (Tables 1 and 2), which indicate that solutes of the size of sucrose should have significantly larger volumes of distribution than inulin. One explanation for this inconsistency is that there is significant extrarenal clearance of sucrose so that the value of A_{tot} (determine by 24 hour urine collection) is underestimated.

For animal studies, the most direct measurement of V_{eq} for solutes with no extrarenal clearance is to nephrectomize the animal and determine the equilibrium concentration after a bolus IV injection. Although this is not an option for humans, a good approximation to this situation can be obtained in subjects with renal failure and very low rates of clearance. For this case, V_{eq} can be estimated from the coefficient of the slow exponential term in the bolus response function (see Methods). Figure 14 shows the good agreement between the predicted venous concentration using a 2-exponential bolus response function and the experimental data of Arancibia et. al. [46] for amoxicillin and Hanna et. al. [47] for morphine-6-glucuronide. Because of the low clearance rate in these subjects, measurements can be extended for longer times (720 minutes for morphine-6-glucuronide and 1440 minutes for amoxicillin) then those used in Table 1. The value of V_{eq} and the time constants for the slow and fast compartments are listed in Table 2. For both solutes, the

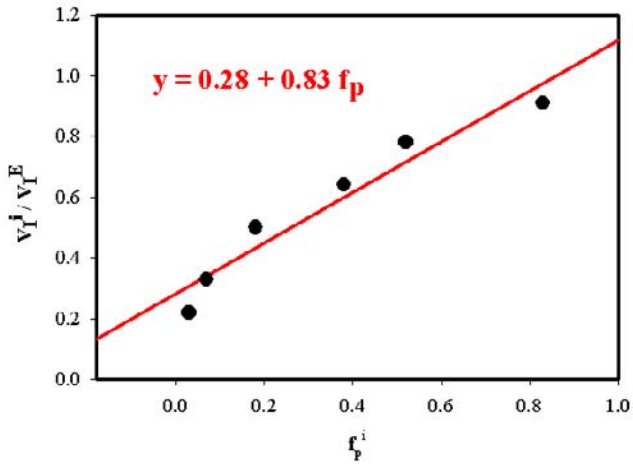

Figure 15
Plot of V_I^i/V_I^E versus f_p^i for the β-lactam antibiotics listed in Table 3. The red line, which is the least squares linear fit to the data, has a slope of 0.83 and intercept of 0.28.

time constant for the slow compartment is about 100 times longer that that for the fast compartment. The time constant of the slow compartment (909 and 2083 minutes) reflects the slow rate of systemic clearance in these subjects. If there were a slowly exchanging compartment that was missed in these subjects, it must have a time constant longer than 900 minutes, which seems unlikely. The values of the "equilibrium" volume of distribution listed in Table 2 are consistent with the values of V_{ss} listed in Table 1 which, as discussed above, should be 5 to 10% too large because of antecubital vein sampling.

The results in Tables 1 and 2 indicate that the extracellular volume of distribution is surprisingly large, about 42% of the total body water. The distribution of this space among the different organs will be discussed in the next section. Tables 1 and 2 also show that the volume of distribution of inulin is about one half the value of the other solutes. This difference is supported by the results of Ladegaard-Pedersen and Engell [48] who found that the inulin volume was, on average, 48% smaller than the EDTA volume in a series of 22 patients. It is ironic that inulin, which is usually regarded as the classical, standard, extracellular marker, seems to be a poor representative of the extracellular space for the typical pharmacokinetic agent. The reduced volume for inulin is presumably produced by the "excluded volume" associated with the interstitial matrix [3], similar to the excluded volume of albumin.

Tissue distribution of interstitial volume (V_I)

Table 4 summarizes the measurements in the literature of the interstitial volumes (V_I) of different organs for a series of extracellular solutes. The value of V_I is expressed as the fraction of the total extravascular organ water. The most striking aspect of the results in this table is the marked variation in V_I for different tissues – varying from about 10 to 15% of total tissue water for skeletal muscle, to 50 to 70% for skin to 80% for tendon. (The high value of 23% for V_I obtained by Bell et. al. [49] in the dog is probably associated with the manipulations required to collect the lymph [50]). The measurements in the dog by Nichols et. al. [51] in 1953 (Table 4) represent the first detailed investigation of the tissue distribution of interstitial volume and form the basis of the current understanding of the extracellular space. These early measurements of Nichols et. al. [51] emphasized the important contribution of connective tissue (represented by tendon) to the total interstitial kinetics [51,52]. In general, the more recent results in Table 4 are in agreement with these earlier measurements.

Volume of distribution of protein bound β-lactam antibiotics

The above discussion has assumed that the test solutes distribute freely in the extracellular blood and tissue water without any binding so that, at equilibrium, the interstitial and plasma concentrations are equal. This is not true if there is blood and/or tissue binding. In this case, the volume of distribution (see eq. (3)) will depend on the degree of tissue binding relative to plasma binding. For the general case, the binding in the different tissues will be unique for each solute, requiring direct tissue binding measurements. However, for the case where the binding is linear and is only due to the plasma and tissue albumin, one can derive (see Appendix, II) the following general relationship for the ratio of the interstitial volume of distribution of solute i (V_I^i) relative to the interstitial EDTA volume of distribution (V_I^E) as a function of f_P^i, the fraction of solute i that is free in plasma:

$$V_I^i / V_I^E = (\alpha_i - K_A) f_P^i + K_A \quad (10)$$

The parameter K_A is the ratio of the albumin concentration in the EDTA interstitial space to the plasma albumin concentration (eq. (9)). The K_A in this equation is for the whole animal and is the weighted average of the K_A^i (see eq. (5)) for the individual organs (see Tables 5 and 6). The parameter α_i is the ratio of the interstitial space for solute i relative to EDTA in the absence of binding. Since EDTA and the β-lactam antibiotics are of similar size, α_i should be close to 1. In the limit of no protein binding ($f_P = 1$), $V_I^i/V_I^E = \alpha_i$. In the limit of very strong binding ($f_P = 0$), $V_I^i/V_I^E = K_A$ (the ratio of tissue to plasma albumin).

Table 3 lists the V_{ss} and V_I of a series of β-lactam antibiotics with varying amounts of plasma protein binding. These antibiotics should satisfy the assumptions required for eq. (10) since they all have linear kinetics and the protein binding results primarily from binding to albumin. Figure 15 shows a plot of V_I^i/V_I^E versus f_p^i for these solutes. (The V_{ss} for flucloxacillin in Table 3 was scaled for an amoxicillin value of 0.26). According to eq. (10), the data points in this plot should fall on a straight line, with a slope of $(\alpha_i - K_A)$ and intercept of K_A. The line in fig. 15, which is the least squares fit to the data points, corresponds to a K_A of 0.28 and an α_i of 1.1. Comparing this value of K_A, which represents a weighted average for the whole animal (eq, (5)), to the value of K_A^i for the individual organs (Table 5) suggest that organs such as skin, tendon and connective tissue dominate the contribution to the total K_A.

PBPK model parameters for extracellular solutes

Based on the physiological data in Tables 1,2,3,4,5, a new set of PBPK parameters was developed that should provide a more accurate description of extracellular solutes, while remaining valid for the other solutes modeled previously by PKQuest. Table 6 (see Methods) summarizes the new PBPK data set. The comparison of the PBPK model predictions using this new parameter set with the experimental data is shown in figures 2,3,4,5,6,7,8,9,10,11,12 for the 11 solutes listed in Tables 1 and 3.

Distributing the extracellular water among the different organs presents something of a conundrum. If one uses the data from Table 4 for the organs that are usually regarded as making up most of the non-fat, non-bone body weight (blood, muscle, skin, gastrointestinal (portal) and liver), one can only account for about 7.3 liters of extracellular water, less than half the total value of about 17.3 liters based on the V_{SS} data in Table 1 (extracellular water equal to 42% of total body water). Since the only other organs of any significant weight are the adipose and connective tissue, these organs must represent a large fraction of the total extracellular water. Connective tissue is very heterogeneous, – consisting of tendons, cartilage, subcutaneous, etc. It is poorly characterized and values for its weight, composition, and blood flow represent, at best, crude estimates. In the classic reference on the extracellular space, Edelman and Leibman [1] estimated that the connective tissue had a mass of 6 Kg and was 70% water (4.2 liters). The fraction of adipose tissue that is extracellular water varies for different locations. One component of the adipose tissue is the subcutaneous component of skin ("subcutis"). In the measurements of Reed et. al. [50] in the rat, subcutis is about 70% water, of which about 51% is extracellular (see Table 4). Adipose tissue in other locations can have much smaller extracellular components. If one assumes that, on average, adipose tissues is 70% lipid and 30% water, then, for the standard human (70 Kg, 20% fat) adipose tissue will contain 6 liters of water.

Based on the above estimates, adipose and connective tissue contain about 10.2 liters of water. For the PBPK model in Table 6, it is assumed that most of this water is extracellular and it is distributed between "adipose" tissue and two connective tissue organs: "tendons" with a relatively low water fraction and low blood flow, and "other" with a higher water fraction and higher blood flow. The total extracellular volume for this PBPK data set is 17.45 liters, or 42% of the total water (Table 6).

As described above (see eq. (10), the interstitial volume of distribution of the β-lactam antibiotics depends on the parameter K_A, the ratio of the albumin concentration in the EDTA interstitial space to the plasma albumin concentration. This value represents the sum over all the different organs. Each individual organ i is characterized by a value of K_A^i. The assumed PBPK values of K_A^i for the different organs are also listed in Table 6. It is assumed that the organs "skin" and "other" have a smaller value of K_A^i then the other organs, consistent with the experimental data in Table 5. The organ-weighted total value of K_A is 0.28 (see Table 6 and eq. (5)), identical to the value obtained by fitting the data in Table 3 (fig. 15).

Capillary Permeability Limitation

Although nearly all PBPK models assume that the blood-tissue exchange for solutes such as EDTA or the β-lactam antibiotics is "flow-limited" (i.e., infinite capillary permeability), there is only indirect evidence to support this assumption. The standard approach that is used to experimentally determine the capillary permeability-surface area product (PS) is the organ perfused early extraction (E_0) method [25]. For an ideal, homogeneous organ, E_0 is equal to the PKQuest parameter "fclear" (see, eq. (6)), the fraction of solute that equilibrates with the tissue in one pass through the capillary [4]. A flow-limited solute has an fclear of 1. As shown in eq. (6), fclear is a function of 3 different physiological parameters: 1) the capillary permeability-surface area product (PS); 2) the organ plasma flow (F); and 3) the fraction of the solute that is free in the plasma (f_P). The standard reference value for the PS of EDTA in skeletal muscle, skin and subcutaneous tissue is about 5 ml/min/100 g [25]. Substituting this value for PS in eq. (6) and using the resting muscle blood flow of 2.25 ml/min/100 gm (Table 6) yields an fclear of 0.89. That is, there is 89% equilibration of EDTA in one pass through the capillary. Since it is difficult to experimentally distinguish an fclear of 0.89 from an fclear of 1 – this result is consistent with the flow limited assumption for EDTA.

There are several uncertainties in this estimate of fclear. To accurately measure PS with the E_0 method it is necessary to use relatively high rates of perfused organ flows so that E_0 (and fclear) are much less than 1. In addition, the E_0 method tends to underestimate the true value of fclear because of factors such as back diffusion and capillary heterogeneity [53,54]. This underestimate is greater for solutes with relatively high permeability, such as EDTA. The two most recent measurements of the skeletal muscle PS of EDTA are 5.0 ml/min/100 g in the cat [55] and 12.9 in rat [54]. Both of these studies have emphasized the importance of using very high blood flows to eliminate the effects of heterogeneity and back diffusion. However, the PS at these high flows (at least 10 times resting flows) may not be relevant to the value of PS at the resting muscle blood flows that are required for the human pharmacokinetic studies. In particular, one would expect that the PS product would be greater at the high flows because the value of S (capillary surface area) would be increased as a result of recruitment of additional capillaries. In addition, the capillaries that are recruited at high flows may not be representative of the low flow capillaries.

The use of the β-lactam antibiotics provides a new approach to the measurement of capillary permeability at resting blood flows [4]. Since the factor f_P multiplies the exponential term in eq. (6), a high protein binding (small f_P) is kinetically equivalent to increasing the blood flow. For example, flucloxacillin, which is 93% bound, has an f_P of 0.07 and a corresponding fclear of 0.15 for a PS of 5 ml/min/100 g and resting muscle blood flow. That is, at resting blood flows only 15% of the plasma flucloxacillin will equilibrate with the tissue in one pass – a large capillary permeability limitation. The use of these protein bound antibiotics allows one to directly measure the capillary permeability at low flows without the uncertainty introduced by heterogeneity and back diffusion.

The approach used in this paper to establish if the antibiotics are flow limited is to determine whether the agreement between the PBPK model and the experimental data was improved by inputting an fclear [muscle] that is less than 1, i.e. a capillary permeability limitation. This is an indirect approach because one would expect that the fit should improve just because another adjustable parameter is introduced. Despite this proviso, there is little doubt that the two antibiotics with the highest degree of protein binding, dicloxacillin (fig. 14, $f_P = 0.03$; fclear = 0.25) and flucloxacillin (fig. 13, $f_P = 0.07$; fclear = 0.344) have a significant capillary permeability limitation. Comparing the PBPK model output for the flow limited and permeability limited conditions in figs. 13 and 14, it can be seen that the primary effect of the permeability limitation is at early times, increasing the initial peak in the plasma concentration. For ceforanide, the third highest binding antibiotic in Table 3 ($f_P = 0.18$, fig. 12), there is a slight improvement in the fit using a fclear [muscle] of 0.52. For the 3 other antibiotics in Table 3, no significant improvement in the fit was obtained by the addition of an fclear, suggesting that they are flow limited. This is consistent with eq. (6) since these antibiotics have an f_P of 0.38 or greater and should have an fclear of greater than 0.7 (assuming a PS = 7, the value obtained for flucloxacillin).

The PBPK estimates of PS of muscle for the β-lactam antibiotics PS are 11.3 ml/min/100 g for dicloxacillin, 7 for flucloxacillin and 5 for ceforanide. Since these three antibiotics have similar structures, one would expect them to have similar PS values. This suggests that the difference in these three PS values provides an indication of the uncertainty in the approach of using PBPK fitting to determine PS. These values are somewhat larger than the recent estimate of Watson [55] for cat skeletal muscle PS of 5 and 7.6 ml/min/100 g for EDTA and mannitol, respectively. These values of Watson [55] were obtained at very high isoproterenol induced blood flows (more than 10 times resting flows) and one would expect these PS values should be greater than the resting PBPK values because of the recruitment of new capillaries and the accompanying increase in capillary surface area. The PBPK value estimated in this paper for the PS of inulin in skeletal muscle is 0.61 ml/min/100 g (see fig. 6) which is in the range of values reported in the literature (0.59 to 1.62 [25]).

The capillary permeability measurements reported here using the PBPK approach are limited by fact that they are whole animal studies. The pharmacokinetics for these extracellular solutes and, therefore, the capillary permeability estimates, are dominated by the organs "skin", "tendon" and "other" which represent 62% of the extravascular water (Table 6). In the implementation in PKQuest, the parameter fclear [muscle] is input, and the fclear of all the other organs are then determined using eq. (6) and a preprogrammed value of PS of each organ relative to muscle. It has been assumed in PKQuest that "skin", "tendon" and "other" have the same PS as skeletal muscle (see Methods).

Despite the quantitative uncertainty in these PS measurements, the qualitative implications are clear. For solutes such as EDTA, mannitol, morphine-6-glucluronide and the weakly bound β-lactam antibiotics, adding the additional factor of a capillary permeability limitation does not significantly improve the fit between the experimental data and the PBPK model prediction. That is, a flow-limited model adequately describes these solutes. In contrast, as predicted using eq. (6), a capillary permeability limitation significantly improves the fit for the highly protein bound β-lactam antibiotics.

Conclusions

In general, each solute that is modeled by PBPK requires unique information about the binding or partition in the individual organs – information that can only by obtained by measurements in animals and then extrapolated to humans. However, this step is not necessary for the extracellular solutes investigated here. Since the solutes do not enter cells, all the diverse cellular binding and uptake processes are circumvented. In addition, if the interstitial binding is primarily due to albumin, as in the case of the β-lactam antibiotics, then the interstitial binding can be predicted just from information about the interstitial albumin concentration (K_A, Table 6). Thus, one can develop a PBPK model or parameter set (Table 6) that is generally applicable to this class of drugs.

This approach is illustrated here for the 11 solutes listed in Tables 1 and 3. A comparison of the model predictions with the experimental data is shown in figs. 2,3,4,5,6,7,8,9,10,11,12. The same PBPK parameter set (Table 6) was used for all of the solutes. The PBPK model predictions shown in these figures were based on the use of only 1 (renal clearance) or 2 (skeletal muscle PS for drugs with high binding) adjustable parameters. In principal, the PS can also be predicted using eq. (6) if an accurate value of f_P is available. Thus, if one knows the systemic clearance for these extracellular solutes, it should be possible to predict the complete time course of the absolute drug concentrations in all the major organs.

Competing Interests

None declared.

Appendix

I. Volume of distribution of 2-compartment model for case where clearance is slow compared to compartment exchange

A two compartment system with a clearance rate constant of k_{10} from the central compartment and exchanges rates of k_{12} and k_{21} between the central and peripheral compartments has the following kinetic solution for the central (venous) concentration c(t) in response to a unit bolus input (V_1 is the volume of the central compartment, D is the bolus dose):

$$C(t) = B_1 e^{-a_1 t} + B_2 e^{-a_2 t}$$

$$a_1 = (1/2)[b + \sqrt{b^2 - 4k_{21}k_{10}}] \qquad a_2 = (1/2)[b - \sqrt{b^2 - 4k_{21}k_{10}}] \tag{A.11}$$

$$B_1 = \frac{D(k_{21} - a_1)}{V_1(a_2 - a_1)} \quad B_2 = \frac{D(k_{21} - a_2)}{V_1(a_1 - a_2)} \qquad b = k_{12} + k_{21} + k_{10}$$

For the special case where the clearance rate constant is small compared to the other exchange rates ($k_{10} << k_{12} + k_{21}$):

$$a_1 \cong k_{12} + k_{21} \qquad a_2 \cong \frac{k_{21}k_{10}}{k_{12} + k_{21}} \qquad B_2 \cong \frac{Dk_{21}}{V_1(k_{12} + k_{21})} \tag{A.12}$$

One can define an "equilibrium volume of distribution" (V_{eq}) for the case where the clearance rate constant (k_{10}) is set to zero and the exchange between the peripheral and central compartment is in equilibrium (A_1 and A_2 are the amounts in the two compartments):

$$k_{12}A_1 = k_{12}V_1 c_{eq} \cong k_{21}A_2 \Rightarrow c_{eq} \cong \frac{k_{21}A_2}{k_{12}V_1}$$

$$A_{tot} = A_1 + A_2 = c_{eq}V_{eq} \Rightarrow V_{eq} \cong V_1 \frac{k_{12} + k_{21}}{k_{21}} \tag{A.13}$$

Substituting this relation for V_{eq} into eq. (A.12) for B_2:

$$V_{eq} \cong D / B_2 \tag{A.14}$$

This expression for V_{eq} is identical to volume of distribution that Wagner [11] defined as V_{dext}:

$$V_{eq} \cong V_{dext} = D / B_\beta \tag{A.15}$$

where B_β is the coefficient of the slow, terminal exponential, determined by extrapolating the terminal component back to time 0, and V_{dext} is the "extrapolated volume of distribution".

II. Derivation of expression for steady state volume of distribution for the case of blood and tissue albumin binding

Definitions:

V_D Steady state volume of distribution

V_P Plasma volume

V_E Interstitial space for EDTA.

V_i Interstitial space for solute i.

λ_E, λ_i Fraction of V_E and V_i that albumin distributes in ($\lambda \leq 1$).

$\alpha_i = V_i/V_E$ ($\alpha_i \geq \lambda_E$).

C_P Total (free + bound) solute concentration in plasma.

c_P, c Free concentration in plasma and tissue.

f_P, f_i, f_0 Fraction of total solute that is free in plasma and tissue and at 0 concentration.

k Albumin binding constant for solute i.

B_P Concentration of protein binding sites in plasma.

B_I Concentration of protein binding sites in interstitial protein space.

$\beta = B_I/B_P$.

$K_A = \beta\lambda_E$

The steady state volume of distribution of solute i (V_D) is define by:

(A.16) $$Amount = V_D C_P = V_P C_P + V_1 C_1 + V_2 C_2$$

where Amount is the total amount of solute in the organ, C_P,C_1 and C_2 are the total (free plus bound) solute concentration in plasma space V_P, in the interstitial space V_1 that albumin distributes in and in the remainder of the interstitial space V_2 available to the solute but not to albumin. Using the above definitions of λ_i, V_1 and V_2 can be related to the interstitial space of solute i (V_i):

(A.17) $$V_1 = \lambda_i V_i \quad V_2 = (1 - \lambda_i)\, V_i$$

Since the total concentration C is related to the free concentration c by C = c/f, and at steady state, c has the same value in all three compartments (assuming removal only from the plasma compartment):

(A.18) $$Amount = \frac{V_D c}{f_P} = \frac{V_P c}{f_P} + \frac{\lambda_i V_i c}{f_i} + (1-\lambda_i) V_i c$$

where f_p and f_i are the fraction of total solute that is free in the plasma and interstitial space, respectively, and it has been assumed there is no protein binding in V_2. Solving (A.18) for V_D:

(A.19) $$V_D = V_P + \delta V_i \qquad \delta = \lambda \frac{f_p}{f_i} + (1-\lambda) f_P$$

The fraction free (f) is related to the protein binding constant (k) and the concentration of protein binding sites (B) by the Scatchard equation:

(A.20) $$f = \frac{1 + kc}{1 + kc + kB}$$

For the case of linear protein binding (no saturation), kc << 1 and δ (eq. (A.19)) is equal to:

(A.21) $$\delta = f_p\,(1 + \lambda k B_I) \qquad (Linear)$$

where B_I is the interstitial protein concentration. For the linear case, the binding constant k in eq. (A.21) can be expressed in terms of f_p and B_p (plasma protein concentration):

(A.22) $$\delta = \beta\lambda_i + f_P\,(1 - \beta\lambda_i) \qquad (Linear)$$

where β is the ratio B_I/B_p. Finally, since the parameters λ_i and V_i depend on the specific solute, they need to be related to some standard value. In PKQuest, the standard is EDTA (λ_E, V_E):

(A.23) $$V_i = \alpha_i V_E \qquad V_{alb} = \lambda_E V_E = \lambda_i V_i \Rightarrow \lambda_i = \frac{\lambda_E}{\alpha_i}$$

Also, it is assumed that $V_i \geq V_{alb}$, and, therefore, $\alpha_i \geq \lambda_E$. Substituting these relations into eqs. (A.22) and (A.19) :

(A.24) $$V_D = V_P + V_E\,[\beta\lambda_E + f_p\,(\alpha_i - \beta\lambda_E)] \qquad (Linear)$$

The interstitial volume of distribution of the bound solute V_I (= V_D-V_P) can then be expressed relative to V_E, the interstitial volume of the EDTA (assumed to have no protein binding):

(A.25) $$V_I / V_E = (\alpha_i - K_A)\, f_p + K_A \qquad K_A = \beta\lambda_E$$

where K_A is the albumin concentration in the EDTA interstitial space divided by the plasma albumin concentration.

III. Modification of differential equations describing PBPK model if the interstitial protein volume is less than the interstitial volume of solute i

In the original derivation for PKQuest [7], it was assumed that the solute and the protein (albumin) distributed in the same interstitial volume. If the protein volume is less than the solute volume, then the differential equation describing the change in total tissue solute concentration (eq. 17 in [7]) must be modified. The total interstitial amount (A_i) of solute i is described by the second two terms on the right side of eq. (A.18):

(A.26) $$\begin{aligned} A_i &= V_i\left[\frac{\lambda_i c_i}{f_i} + (1-\lambda_i)c_i\right] = V_i\left[\lambda_i\left(c_i + \frac{kB_I}{1+kc_i}\right) + (1-\lambda_i)c_i\right] \\ &= V_i\left(c_i + \frac{k\lambda_i B_I c_i}{1+kc_i}\right) = V_i(c_i + c_b) \qquad c_b = \frac{k\lambda_i B_I c_i}{1+kc_i} \end{aligned}$$

where c_i and c_b are the free and bound tissue concentrations of solute i and eq. (A.20) has been substituted for f_i. Comparing the expression for c_b in eq. (A.26) with the original expression (eq. 16 in [7]), it can be seen that the only modification that is required is the substitution of $\lambda_i B_I$ in place of B_I.

In the implementation in PKQuest the interstitial binding in organ j is characterized by the following set of parameters:

ecf [j]: interstitial EDTA volume as fraction of total organ water.

frecf [j,i]: = α_i = interstitial space of solute i as fraction of EDTA space

cProt [j]: = $K_A^j = \beta\lambda_E$

$\lambda_i B_I = cProt * B_p / frecf$

Additional material

Additional File 1

"PKQuest_worksheets.doc" *– Contains the complete PKQuest Maple worksheets for the 11 solutes modeled in figs. 2,3,4,5,6,7,8,9,10,11,12.*
Click here for file
[http://www.biomedcentral.com/content/supplementary/1472-6904-3-3-S1.doc]

Acknowledgements

I wish to thank Dr Mike Laker for providing additional information about an experimental subject in his published paper.

References

1. Edelman IS and Liebman J: **Anatomy of body water and electrolytes.** *American Journal of Medicine* 1959, **27:**256-275.
2. Aukland K and Nicolaysen G: **Interstitial fluid volume: local regulatory mechanisms.** *Physiol Rev* 1981, **61:**556-643.
3. Bert JL and Pearce RH: **The interstitium and microvascular exchange.** In: *Hanbook of Physiology, The Cardiovascular System Microcirculation, Part I Volume IV*. Edited by: *Renkin EM, Michel CC. Bethesda, MD: American Physiological Society*; 1984:521-547.
4. Levitt DG: **PKQuest: capillary permeability limitation and plasma protein binding – application to human inulin, dicloxacillin and ceftriaxone pharmacokinetics.** *BMC Clin Pharmacol* 2002, **2:**7.
5. Levitt DG: **PKQuest: volatile solutes – application to enflurane, nitrous oxide, halothane, methoxyflurane and toluene pharmacokinetics.** *BMC Anesthesiol* 2002, **2:**5.
6. Levitt DG: **PKQuest: measurement of intestinal absorption and first pass metabolism – application to human ethanol pharmacokinetics.** *BMC Clin Pharmacol* 2002, **2:**4.
7. Levitt DG: **PKQuest: a general physiologically based pharmacokinetic model. Introduction and application to propranolol.** *BMC Clin Pharmacol* 2002, **2:**5.
8. Levitt DG: **The use of a physiologically based pharmacokinetic model to evaluate deconvolution measurements of systemic absorption.** *BMC Clin Pharmacol* 2003, **3:**1.
9. Tsuji A, Yoshikawa T, Nishide K, Minami H, Kimura M, Nakashima E, Terasaki T, Miyamoto E, Nightingale CH and Yamana T: **Physiologically based pharmacokinetic model for beta-lactam antibiotics I: Tissue distribution and elimination in rats.** *J Pharm Sci* 1983, **72:**1239-52.
10. Rominger KL and Wolf M: **A critical view of distribution volumes.** In: *Pharmacokinetics during drug development: data analysis and evaluation techniques* Edited by: *Bozler G, van Rossum JM. Stuttgart: Gustav Fischer Verlag*; 1982:45-64.
11. Wagner JG: **Linear pharmacokinetic equations allowing direct calculation of many needed pharmacokinetic parameters from the coefficients and exponents of polyexponential equations which have been fitted to the data.** *J Pharmacokinet Biopharm* 1976, **4:**443-67.
12. Snyder WS and ed: *Report of the task group on refereance man Oxford: Pergamon Press*; 1975.
13. Jonsson F and Johanson G: **Physiologically Based Modeling of the Inhalation Kinetics of Styrene in Humans Using a Bayesian Population Approach.** *Toxicol Appl Pharmacol* 2002, **179:**35-49.
14. Chumlea WC, Guo SS, Zeller CM, Reo NV, Baumgartner RN, Garry PJ, Wang J, Pierson RN Jr, Heymsfield SB and Siervogel RM: **Total body water reference values and prediction equations for adults.** *Kidney Int* 2001, **59:**2250-8.
15. Williams LR and Leggett RW: **Reference values for resting blood flow to organs of man.** *Clin Phys Physiol Meas* 1989, **10:**187-217.
16. Schloerb PR, Friis-Hansen BJ, Edelman IS, Solomon AK and Moore FD: **The measurement of total body water in the human subject by deuterium oxide dilution.** *J Clin Invest* 1950, **29:**1296-310.
17. Laine H, Yki-Jarvinen H, Kirvela O, Tolvanen T, Raitakari M, Solin O, Haaparanta M, Knuuti J and Nuutila P: **Insulin resistance of glucose uptake in skeletal muscle cannot be ameliorated by enhancing endothelium-dependent blood flow in obesity.** *J Clin Invest* 1998, **101:**1156-62.
18. Eriksson JW, Smith U, Waagstein F, Wysocki M and Jansson PA: **Glucose turnover and adipose tissue lipolysis are insulin-resistant in healthy relatives of type 2 diabetes patients: is cellular insulin resistance a secondary phenomenon?** *Diabetes* 1999, **48:**1572-8.
19. Elia M and Kurpad A: **What is the blood flow to resting human muscle?** *Clin Sci (Lond)* 1993, **84:**559-63.
20. Munson ES, Eger EI 2nd, Tham MK and Embro WJ: **Increase in anesthetic uptake, excretion, and blood solubility in man after eating.** *Anesth Analg* 1978, **57:**224-31.
21. Virtanen KA, Lonnroth P, Parkkola R, Peltoniemi P, Asola M, Viljanen T, Tolvanen T, Knuuti J, Ronnemaa T, Huupponen R and Nuutila P: **Glucose uptake and perfusion in subcutaneous and visceral adipose tissue during insulin stimulation in nonobese and obese humans.** *J Clin Endocrinol Metab* 2002, **87:**3902-10.
22. Tothill P and Hooper G: **Measurement of tendon blood flow in rabbits by microsphere uptake and 133Xe washout.** *J Hand Surg [Br]* 1985, **10:**17-20.
23. Riggi K, Wood MB and Ilstrup DM: **Dose-dependent variations in blood flow evaluation of canine nerve, nerve graft, tendon, and ligament tissue by the radiolabeled-microsphere technique.** *J Orthop Res* 1990, **8:**909-16.
24. Grimby G, Nilsson NJ and Sanne H: **Serial determinations of cardiac output at rest.** *Br Heart J* 1966, **28:**118-21.
25. Crone C and Levitt DG: *Capillary permeability to small solutes Bethesda, Maryland: American Physiological Society*; 1984.
26. Lossius K, Eriksen M and Walloe L: **Fluctuations in blood flow to acral skin in humans: connection with heart rate and blood pressure variability.** *J Physiol* 1993, **460:**641-55.
27. Chiou WL: **The phenomenon and rationale of marked dependence of drug concentration on blood sampling site. Implications in pharmacokinetics, pharmacodynamics, toxicology and therapeutics (Part I).** *Clin Pharmacokinet* 1989, **17:**175-99.
28. Sutherland R, Croydon EA and Rolinson GN: **Amoxycillin: a new semi-synthetic penicillin.** *Br Med J* 1972, **3:**13-6.
29. Wise R, Gillett AP, Cadge B, Durham SR and Baker S: **The influence of protein binding upon tissue fluid levels of six beta-lactam antibiotics.** *J Infect Dis* 1980, **142:**77-82.
30. Lode H, Elvers A, Koeppe P and Borner K: **Comparative pharmacokinetics of apalcillin and piperacillin.** *Antimicrob Agents Chemother* 1984, **25:**105-8.
31. Pfeffer M, Gaver RC and Ximenez J: **Human intravenous pharmacokinetics and absolute oral bioavailability of cefatrizine.** *Antimicrob Agents Chemother* 1983, **24:**915-20.
32. Pfeffer M, Gaver RC and Van Harken DR: **Human pharmacokinetics of a new braod-spectrum parenteral cephalosporin antibiotic, ceforanide.** *J Pharm Sci* 1980, **69:**398-403.
33. Roder BL, Frimodt-Moller N, Espersen F and Rasmussen SN: **Dicloxacillin and flucloxacillin: pharmacokinetics, protein binding and serum bactericidal titers in healthy subjects after oral administration.** *Infection* 1995, **23:**107-12.
34. Van Crugten JT, Sallustio BC, Nation RL and Somogyi AA: **Renal tubular transport of morphine, morphine-6-glucuronide, and**

morphine-3-glucuronide in the isolated perfused rat kidney. *Drug Metab Dispos* 1991, **19:**1087-92.
35. Wiig H, Kaysen GA, al-Bander HA, De Carlo M, Sibley L and Renkin EM: **Interstitial exclusion of IgG in rat tissues estimated by continuous infusion.** *Am J Physiol* 1994, **266:**H212-9.
36. Johnson JA: **Capillary permeability, extracellular space estimation, and lymph flow.** *Am J Physiol* 1966, **211:**1261-3.
37. Odeh YK, Wang Z, Ruo TI, Wang T, Frederiksen MC, Pospisil PA and Atkinson AJ Jr: **Simultaneous analysis of inulin and 15N2-urea kinetics in humans.** *Clin Pharmacol Ther* 1993, **53:**419-25.
38. Orlando R, Floreani M, Padrini R and Palatini P: **Determination of inulin clearance by bolus intravenous injection in healthy subjects and ascitic patients: equivalence of systemic and renal clearances as glomerular filtration markers.** *Br J Clin Pharmacol* 1998, **46:**605-9.
39. Ladegaard-Pedersen HJ: **Measurement of extracellular volume and renal clearance by a single injection of inulin.** *Scand J Clin Lab Invest* 1972, **29:**145-53.
40. Prescott LF, McAuslane JA and Freestone S: **The concentration-dependent disposition and kinetics of inulin.** *Eur J Clin Pharmacol* 1991, **40:**619-24.
41. Nassberger L and DePierre JW: **Uptake, distribution and elimination of 3H-gentamicin in different organs of the rat as determined by scintillation counting.** *Acta Pharmacol Toxicol (Copenh)* 1986, **59:**356-61.
42. Penson RT, Joel SP, Roberts M, Gloyne A, Beckwith S and Slevin ML: **The bioavailability and pharmacokinetics of subcutaneous, nebulized and oral morphine-6-glucuronide.** *Br J Clin Pharmacol* 2002, **53:**347-54.
43. Ludden TM, Beal SL and Sheiner LB: **Comparison of the Akaike Information Criterion, the Schwarz criterion and the F test as guides to model selection.** *J Pharmacokinet Biopharm* 1994, **22:**431-45.
44. Schwartz IL, Schacthter D and Freinkel N: **The measurement of extracellular fluid in man by means of a constant infusion technique.** *Journal of Clinical Investigaton* 1945, **28:**1117-1125.
45. Deane N, Schreiner GE and Robertson JS: **The velocity of distribution of sucrose between the plasma and interstitial fluid, with reference to the use of sucrose for the extracellular fluid in man.** *J Clin Investigation* 1951, **30:**1463-1468.
46. Arancibia A, Drouguett MT, Fuentes G, Gonzalez G, Gonzalez C, Thambo S and Palombo G: **Pharmacokinetics of amoxicillin in subjects with normal and impaired renal function.** *Int J Clin Pharmacol Ther Toxicol* 1982, **20:**447-53.
47. Hanna MH, D'Costa F, Peat SJ, Fung C, Venkat N, Zilkha TR and Davies S: **Morphine-6-glucuronide disposition in renal impairment.** *Br J Anaesth* 1993, **70:**511-4.
48. Ladegaard-Pedersen HJ and Engell HC: **A comparison of the distribution volumes of inulin and (51 Cr)EDTA in man and nephrectomized dogs.** *Scand J Clin Lab Invest* 1972, **30:**267-70.
49. Bell DR, Watson PD and Renkin EM: **Exclusion of plasma proteins in interstitium of tissues from the dog hind paw.** *Am J Physiol* 1980, **239:**H532-H538.
50. Reed RK, Lepsoe S and Wiig H: **Interstitial exclusion of albumin in rat dermis and subcutis in over- and dehydration.** *Am J Physiol* 1989, **257:**H1819-27.
51. Nichols G, Nichols N, Weil WB and Wallace WM: **The direct measurement of the extracellular phase of tissues.** *J Clinical Investigation* 1953, **32:**1299-1308.
52. Kruhoffer P: **Inullin as an indicator for the extracellular space.** *Acta Physiol Scand* 1946, **11:**16-36.
53. Bass L: **Flow dependence of first-order uptake of substances by heterogeneous perfused organs.** *J Theor Biol* 1980, **86:**365-76.
54. Haraldsson B and Rippe B: **Restricted diffusion of CrEDTA and cyanocobalamine across the exchange vessels in rat hindquarters.** *Acta Physiol Scand* 1986, **127:**359-72.
55. Watson PD: **Permeability of cat skeletal muscle capillaries to small solutes.** *Am J Physiol* 1995, **268:**H184-93.
56. Cousins C, Mohammadtaghi S, Mubashar M, Strong R, Gunasekera RD, Myers MJ and Peters AM: **Clearance kinetics of solutes used to measure glomerular filtration rate.** *Nucl Med Commun* 1999, **20:**1047-54.
57. Laker MF, Bull HJ and Menzies IS: **Evaluation of mannitol for use as a probe marker of gastrointestinal permeability in man.** *Eur J Clin Invest* 1982, **12:**485-91.
58. Elia M, Behrens R, Northrop C, Wraight P and Neale G: **Evaluation of mannitol, lactulose and 51Cr-labelled ethylenediaminetetra-acetate as markers of intestinal permeability in man.** *Clin Sci (Lond)* 1987, **73:**197-204.
59. Lotsch J, Weiss M, Kobal G and Geisslinger G: **Pharmacokinetics of morphine-6-glucuronide and its formation from morphine after intravenous administration.** *Clin Pharmacol Ther* 1998, **63:**629-39.
60. Penson RT, Joel SP, Clark S, Gloyne A and Slevin ML: **Limited phase I study of morphine-3-glucuronide.** *J Pharm Sci* 2001, **90:**1810-6.
61. Sjovall J, Westerlund D and Alvan G: **Renal excretion of intravenously infused amoxycillin and ampicillin.** *Br J Clin Pharmacol* 1985, **19:**191-201.
62. Arancibia A, Guttmann J, Gonzalez G and Gonzalez C: **Absorption and disposition kinetics of amoxicillin in normal human subjects.** *Antimicrob Agents Chemother* 1980, **17:**199-202.
63. Lofgren S, Bucht G, Hermansson B, Holm SE, Winblad B and Norrby SR: **Single-dose pharmacokinetics of dicloxacillin in healthy subjects of young and old age.** *Scand J Infect Dis* 1986, **18:**365-9.
64. Wiig H, DeCarlo M, Sibley L and Renkin EM: **Interstitial exclusion of albumin in rat tissues measured by a continuous infusion method.** *Am J Physiol* 1992, **263:**H1222-33.
65. Wiig H, Reed RK and Tenstad O: **Interstitial fluid pressure, composition of interstitium, and interstitial exclusion of albumin in hypothyroid rats.** *Am J Physiol Heart Circ Physiol* 2000, **278:**H1627-39.
66. Wiig H and Lund T: **Relationship between interstitial fluid volume and pressure (compliance) in hypothyroid rats.** *Am J Physiol Heart Circ Physiol* 2001, **281:**H1085-92.
67. Rippe C, Rippe B and Erlanson-Albertsson C: **Capillary diffusion capacity and tissue distribution of pancreatic procolipase in rat.** *Am J Physiol* 1998, **275:**G1179-84.
68. Larsson M, Johnson L, Nylander G and Ohman U: **Plasma water and 51Cr EDTA equilibration volumes of different tissues in the rat.** *Acta Physiol Scand* 1980, **110:**53-7.
69. Katz J, Bonorris G, Golden S and Sellers AL: **Extravascular albumin mass and exchange in rat tissues.** *Clin Sci* 1970, **39:**705-24.
70. Barratt TM and Walser M: **Extracellular volume in skeletal muscle of the rat and dog: a comparison of radiosulphate and radiobromide spaces.** *Clin Sci* 1968, **35:**525-36.
71. Holmang A, Bjorntorp P and Rippe B: **Tissue uptake of insulin and inulin in red and white skeletal muscle in vivo.** *Am J Physiol* 1992, **263:**H1170-6.
72. Mullins RJ, Powers MR and Bell DR: **Albumin and IgG in skin and skeletal muscle after plasmapheresis with saline loading.** *Am J Physiol* 1987, **252:**H71-9.
73. Poole-Wilson PA and Cameron IR: **ECS, intracellular pH, and electrolytes of cardiac and skeletal muscle.** *Am J Physiol* 1975, **229:**1299-1304.
74. Wittmers LE Jr, Bartlett M and Johnson JA: **Estimation of the capillary permeability coefficients of inulin in various tissues of the rabbit.** *Microvasc Res* 1976, **11:**67-78.
75. Wiig H and Reed RK: **Interstitial compliance and transcapillary Starling pressures in cat skin and skeletal muscle.** *Am J Physiol* 1985, **248:**H666-73.
76. Wiig H and Reed RK: **Volume-pressure relationship (compliance) of interstitium in dog skin and muscle.** *Am J Physiol* 1987, **253:**H291-8.
77. Sjogaard G and Saltin B: **Extra- and intracellular water spaces in muscles of man at rest and with dynamic exercise.** *Am J Physiol* 1982, **243:**R271-80.
78. Reinoso RF, Telfer BA and Rowland M: **Tissue water content in rats measured by desiccation.** *J Pharmacol Toxicol Methods* 1997, **38:**87-92.
79. Mullins RJ and Bell DR: **Changes in interstitial volume and masses of albumin and IgG in rabbit skin and skeletal muscle after saline volume loading.** *Circ Res* 1982, **51:**305-13.

Pre-publication history

The pre-publication history for this paper can be accessed here:

http://www.biomedcentral.com/1472-6904/3/3/prepub